Improving Pipeline Safety During Gas Leakage Events Using Near Real-Time Data Networks and Optimal Decision-Making Tools

November 30, 2020 – August 31, 2023

Grant No. 693JK32050005CAAP

Summary Report

In Partnership with The University of Texas at Arlington, Colorado State University and Southern Methodist University

Kathleen M. Smits, Jui-Hsiang Lo, Daniel J. Zimmerle, and Gerald P. Duggan

Legal Notice

This research was funded in part under the Department of Transportation (DOT), Pipeline and Hazardous Materials Safety Administration's (PHMSA) Pipeline Safety Research and Development Program (Project#: 897). The views and conclusions contained in this document are those of the authors and should not be interpreted as representing the official policies, either expressed or implied, of the Pipeline and Hazardous Materials Safety Administration, or the U.S. Government.

Acknowledgments

The project team would like to thank PHMSA for providing funding to perform this research. The research would not have been possible without the help of industry partners to include Southern California Gas Company, ConsolidatedEdison, Xcel Energy, and Pacific Gas and Electric. In addition, special thanks to industry partners who provided essential site access and data.

Table of Contents

Table of Figures

Table of Tables

List of Acronyms

- CH_4 - Methane
- CSU – Colorado State University
- DOE – Department of Energy
- DP-IR+ – DetectoPak Infrared (Heath Consultants, Inc.)
- METEC – Methane Emission Technology Evaluation Center
- MONITOR – Methane Observation Networks with Innovative Technology to Obtain Reductions
- NG – Natural Gas
- UTA – University of Texas at Arlington

Executive Summary

This project was in response to NOFO # 693JK320NF0001, focusing on Research Area #1: Pipeline Safety Academic Collaboration with Industry. The primary objective was the improvement of the safety of urban and rural natural gas transportation and distribution systems by developing an innovative real-time decision-making algorithm for methane detection and quantification of belowground leaks. To accomplish the project's objectives, five tasks were outlined with specific deliverables and activities. The work was conducted with a combined team of researchers from Colorado State University and the University of Texas at Arlington and in partnership with Southern Methodist University.

A collaborative study structure was established between UTA, CSU, industry collaborators, and regulatory advisors. Meetings were initially planned in person but due to the COVID-19 restrictions, most meetings were moved to online. However, field research and the last year of project meetings were predominantly in person. Through the partnership, a more comprehensive understanding of distribution pipeline leaks was obtained. The information provided was used to plan experiments and develop the CH_4 detector network and algorithm to quantify non-steady state leakage from belowground pipelines.

Through the partnership, a more comprehensive understanding of leak response operational practices was established, specifically regarding gas migration from underground pipeline leakage. The influence of the subsurface and surface environment linked to variability in atmospheric conditions and soil characteristics was identified and further investigated through field experiments and numerical modeling.

A low-cost, near real-time, wireless natural gas monitoring detector network was developed to link the near real-time data from CH_4 detectors, on-site weather sensors, and soil moisture and temperature sensor. The CH_4 detector was modified based on a prior design of a low-cost CH_4 sensor [Cho et al., 2022] to monitor surface and belowground near-surface gas concentrations. The depth of belowground measurement was 1.2 cm below the ground surface. The on-site weather sensor and soil moisture temperature sensor were utilized to measure the variation of atmospheric variability (e.g., wind speed, air temperature, and solar radiation) and soil characteristics (i.e., soil moisture and temperature). Measurements could be transmitted to the network database by wire or wireless approach. The data in the database was used in the inverse gas migration model for the quantification of non-steady belowground NG leak rates. In this project, nineteen low-cost, near real-time CH_4 detectors were produced and used to monitor the change in surface and belowground near-surface CH_4 concentrations with the stepwise controlled NG leak rates in a permeable (soil and grass) area. Deploying the low-cost, near-real-time CH_4 detector around the area with the highest surface CH_4 concentration proved to be an effective strategy for determining pipeline leak rates in field applications.

Through a series of field-scale controlled NG experiments with gas leakage rates varying in size from 37 to 121 g/h, we captured the spatial and temporal distribution of surface and belowground near-surface (BNS) CH_4 concentrations and surrounding environmental data continuously over time. Data was used in a model to estimate the changes in NG leak rate over time. The model was developed based on a previous model (Estimating the Surface Concentration Above Pipeline Emission, ESCAPE) that was used to estimate surface CH_4 enhancements above a leak using selected environmental and

leak data as input. The model was modified to incorporate the impact of belowground soil properties on gas migration to account for the steady and non-steady state gas behaviors in the event of a leak rate change. Experimental results indicate that elevated BNS gas concentrations persist long before elevated surface concentrations are observed. On average, BNS CH_4 concentrations (1.2 cm below the soil surface) were higher than average surface concentrations with the range from 20% to 486% within a monitoring radius of 4 meters. In addition, with an increase in the leak rate from 37 to 84 g/h, an increase in the BNS CH_4 concentration was observed within 3 hours with an increasing leak rate. However, due to the influence of atmospheric fluctuations, any changes in surface CH_4 concentrations could not be confirmed within this period. Over longer periods (e.g., 1.5 days), the plume area of the BNS CH_4 extended approximately two times farther than that of the surface CH_4 as the gas leak rate increased from 37 (g/h) to 121 (g/h). The modified ESCAPE model was able to capture changes in gas leakage, agreeing well with the experimental NG leak rates (m=0.99 and R^2=0.77). The improvement by the modified ESCAPE model indicated that including soil characteristics and BNS CH_4 measurements can advance estimations of non-steady NG leak rates in low and moderate NG leak rate scenarios (leaks from 37 to 121 g/h). Therefore, the proposed low-cost near-real-time CH_4 detector network and the modified ESCAPE model in this study provide an innovative tool for the industry to not only support the understanding of NG leakage events to respond to gas leaks efficiently and safely but also improve operators' risk assessments for addressing and preventing gas leakage incidents.

Opportunities for postdoctoral researcher and student training and development were provided as part of this work. 1 postdoctoral researcher, 2 graduate and 5 undergraduate engineering students from diverse backgrounds were supported, in part, by this research. Students went on to persue positions in various engineering firms (4) and continuing graduate studies (4).

Based on the findings presented in this project, we propose several areas for further research. First, investigating the spatial and temporal variations of soil moisture and temperature is essential to enhance our understanding of subsurface gas migration in diverse soil conditions. Second, the work presented here did not include the impact of precipitation, soil layering and significant changes in soil moisture on the model output. Additional diverse conditions need to be tested to broaden the applicability of this approach. Lastly, conducting controlled gas release experiments in line with the suggested scenarios in this report is recommended. This will provide valuable insights for refining the practice of the low-cost, near real-time CH_4 network and the modified ESCAPE model in detecting and estimating belowground NG leak rates. By expanding the scope of these experiments to include different scenarios, we can gain a deeper understanding of the optimal number of measured locations and times required for precise leak rate estimation. In summary, further research in these areas will contribute to advancing our knowledge and improving the accuracy of quantifying belowground NG leak rates. In the end, in addition to the conditions tested here, many other factors, such as investigating the effect of trenched bed systems or fractured soils, vegetation or surface/subsurface obstructions, and varying atmospheric conditions on gas migration, should be included in the analysis of gas leakage scenarios to improve industry best practices.

Introduction

Background and Objectives

Natural gas (NG) pipeline safety has made significant advancements in recent decades; however, incidents of leakage persist, often attributed to aging infrastructure, excavation activities, and human errors. The consequences of pipeline leakage can be catastrophic, involving the accumulation and migration of gas through subsurface environments, ultimately leading to its release into the atmosphere or substructures such as basements, French drains, or sewer lines. The Pipeline and Hazardous Material and Safety Administration's (PHMSA) reported that pipeline leakage resulted in 1,030 injuries between 2002 and 2021, with 6 from gathering lines, 157 from transmission lines, and 867 from distribution lines [PHMSA, 2022].

Despite advancements in methane detection technology, effectively addressing subsurface pipeline leaks remains challenging due to their complex nature and extent. Subsurface NG migration is heavily influenced by soil layers, surrounding subsurface infrastructure, gas composition, and pipeline pressures. Surface conditions, including pavements and buildings (e.g., basements and crawlspaces), can impede gas flow and its release into the atmosphere, potentially leading to lateral transport or underground accumulation. Additionally, NG migration is impacted by pressure differentials arising from short-term fluctuations in barometric pressure due to atmospheric wind oscillations [Dufrane et al., 2017], long-term meteorological changes in barometric pressure [Bleem et al, 2019], and water table fluctuations caused by site-specific hydrogeology or rainfall events [Duggan et al., 2015]. These factors contribute to a dynamic and intricate environment for leak detection and quantification.

In both urban and rural environments, utilities face three concerns that a remote near real-time monitoring and decision-making tool could assist with (1) the need to monitor a repaired leak site to ensure aeration operations are properly decreasing belowground gas concentrations (2) the need to monitor an active construction site where belowground digging is actively occurring to ensure pipeline integrity (3) the need to monitor a known leak that cannot be repaired immediately for some reason. For instance, a Grade 3 leak may be upgraded to a Grade 2 leak during the prolonged delay between detection and repair (typically, state regulations require Grade 2 leaks to be fixed within 12-15 months from detection/reporting). Although practices are in place to periodically reevaluate existing leaks (e.g., every 3-6 months), changes in leak significance can occur between reevaluation periods due to various factors, such as concurrent utility or construction work, variations in soil moisture conditions, or alterations in surface structures. This issue is particularly pertinent in urban areas. Another example is the need to monitor an aeration site after a leak repair. Soil gas concentrations can oftentimes persist in such scenarios for multiple days, requiring active monitoring by operators. Therefore, there is a clear need for remote monitoring capabilities to track the behavior of repaired and actively aerating and existing gas leaks over time, enabling the detection of any changes not only in gas concentration but also in leakage rate, indicating potential variations in leak size or location. Additionally, continuous efforts are required to prevent hazardous leaks and safeguard properties by monitoring aging infrastructure and areas with competing utilities or ongoing construction work, as these circumstances may result in the recurrence or simultaneous occurrence of multiple leaks. Gas detectors should be deployed in a network on the soil surface around suspected leak locations or within boreholes to capture aboveground and belowground gas concentrations. However, the current lack of cost-effective gas monitoring and decision-making solutions hinders the timely localization and quantification of leaks. Thus, an effective methane detector network could inform predictions on gas leakage behavior, as well

as repair and response strategies. Most CH_4 detection solutions currently available only provide information on gas concentration at specific locations and times, lacking the ability to capture dynamic changes influenced by environmental conditions. Therefore, a low-cost, long-term, real-time monitoring network is necessary for operators to monitor and quantify belowground NG leak rates.

The main objective of this project was to develop a low-cost, near real-time, wireless natural gas monitoring detector network linked with a leak quantification algorithm that can provide operators with decision-making information related to gas leakage incidents. This project:

- Develops a low-cost, near real-time, wireless natural gas monitoring detector network to provide operators with decision-making information related to gas leakage incidents.
- Develops a method to process data collected in a network, resulting in a gas-sensing protocol.
- Provides a recommended practice to deploy the gas sensing protocol.
- Advances the science of leak detection and measurement methods for underground pipelines.

Scope of work

The project was divided into five main tasks: 1) Establish a collaborative study structure with InSeNSE advisors; 2) Develop the low-cost near real-time CH_4 detector network and simulation-approach; 3) Conduct controlled NG release experiments; 4) Conduct field validation of the approach with a local utility company; and 5) Provide a recommended practice of proposed CH_4 detector network and the approach.

- Task 1: The collaborative study structure was established between the University of Texas at Arlington (UTA), Colorado State University (CSU), and Southern Methodist University (SMU). SMU was included towards the end of the project due to the PIs relocation. This close partnership played a pivotal role in the success of the project, as it facilitated continuous interaction and ensured that the project deliverables and approach aligned with the requirements of the funding entity. To maintain effective communication and progress tracking, quarterly virtual meetings and reports were conducted throughout the project. In addition, the UTA/CSU/SMU project team performed field experiments with operators and had multiple update meetings during the project. These regular engagements provided opportunities to discuss updates, address any challenges, and ensure that the project remained on track toward its objectives.
- Task 2: The objective of Task 2 was to develop a low-cost near real-time CH_4 detector network that linked multiple sensors to a simulation model. The network aimed to capture the spatial and temporal distribution of surface and belowground near-surface gas concentrations and quantify non-steady belowground NG leak rates. The simulation model used in this project was a modified version of the Estimating the Surface Concentration Above Pipeline Emissions (ESCAPE) model, which provides surface gas emission estimates based on known leak location and atmospheric conditions. The modified

ESCAPE model integrated belowground near-surface gas measurements and soil characteristics with the original ESCAPE model to improve the estimation of belowground NG leak rates.

- Task 3: Multiple controlled NG release experiment was conducted at the Methane Emission Technology Evaluation Center (METEC), Fort Collins, CO. The first set of experiments (year 1) tested the wireless detector network and various layout scenarios. This was followed by a 7-day experiment that tested the wireless detector network linked with the optimal decision-making algorithm for gas leakage. A third set of experiments tested more scenarios with various layouts (e.g. pavement). Experiments were designed to collect data at relevant space and time scales for each scenario.
- Task 4: Field experiments were performed with an industry partner. The algorithm developed in this project was evaluated for a wide range of field applications. The leak rates determined by the algorithm were compared with the measurements from an industry-standard method (i.e. flux chamber approach). Seven field experiments carried out in this project ensured the application of the algorithm to a wide range of pipeline leakage scenarios.
- Task 5: Results of Tasks 2 to 4 were used to establish suggested scenarios for deploying the detectors to properly detect and quantify the non-steady belowground NG leak rate in complicated environments. This was completed in cooperation with the project guidance committee.

Document Organization

The document is organized into six sections based on the project deliverables and key activities.

- Deliverable 1: Development of low-cost, near-real-time, wire/wireless natural gas detector network.
- Deliverable 2: Comprehensive experimental data sets from METEC test site
- Deliverable 3: Field Experiments with the industry partner
- Deliverable 4: The inversion algorithms for quantifying the belowground NG leak rates – Modified ESCAPE model.
- Deliverable 5: Recommended to incorporate findings into practice.
- Deliverable 6: Project Outputs – Findings are published in conference presentations and peer-reviewed journals which can be accessed via deliverable 4. Student workforce development is also discussed.

Deliverable 1: Development of Low-cost, Near-real-time, Wire/Wireless Natural Gas Detector Network

Objective

Developing a network of low-cost, near real-time, wireless CH_4 detectors linking monitoring of surface/belowground gas concentrations, weather conditions, and soil moisture/temperature to an inverse gas migration model to establish a comprehensive system for effectively tracking and quantifying belowground NG leak rates.

Framework of the CH_4 detector network

The conceptual framework of the low-cost, near real-time, wireless CH_4 detector network is shown in Figure 1. The detector network consists of low-cost near real-time CH_4 detectors, soil moisture and temperature sensors (5TM, METER Group, Inc.), and a weather sensor (ATMOS 41, METER Group, Inc.). Controlling software in the CH_4 detector was used to transfer collected measurements of CH_4 concentrations via wire and wireless connection.

The CH_4 detector is used to monitor surface and belowground near-surface CH4 concentrations and the surrounding air temperature, air pressure, and relative humidity. The variations in the environmental CH_4 concentration induce the change in the voltage in the detector. This change in voltage and measured relative humidity and air temperature are used to calculate CH_4 concentration [Cho et al., 2022]. Meteorological and soil conditions are collected using data loggers and then transferred wirelessly to the network database. Furthermore, the background CH_4 concentration in the atmosphere, the depth of the pipeline, and the location of potential leak determined by the handheld detector (e.g., DP-IR+) are investigated and then transferred wirelessly to the network database. These data are used to calculate the required parameters in the modified ESCAPE model. The required parameters include atmospheric and soil resistances and spatial-temporal distribution of CH_4 concentration. Parameters are then input into the modified ESCAPE model to estimate the non-steady belowground NG leak rate. The collected data and simulated results from the modified ESCAPE model are uploaded to a user website that can be used to (1) visualize the gas concentration spatially over time or (2) understand the model estimates of leak rate over time. Details about used detectors and sensors in the network are described in the following sections.

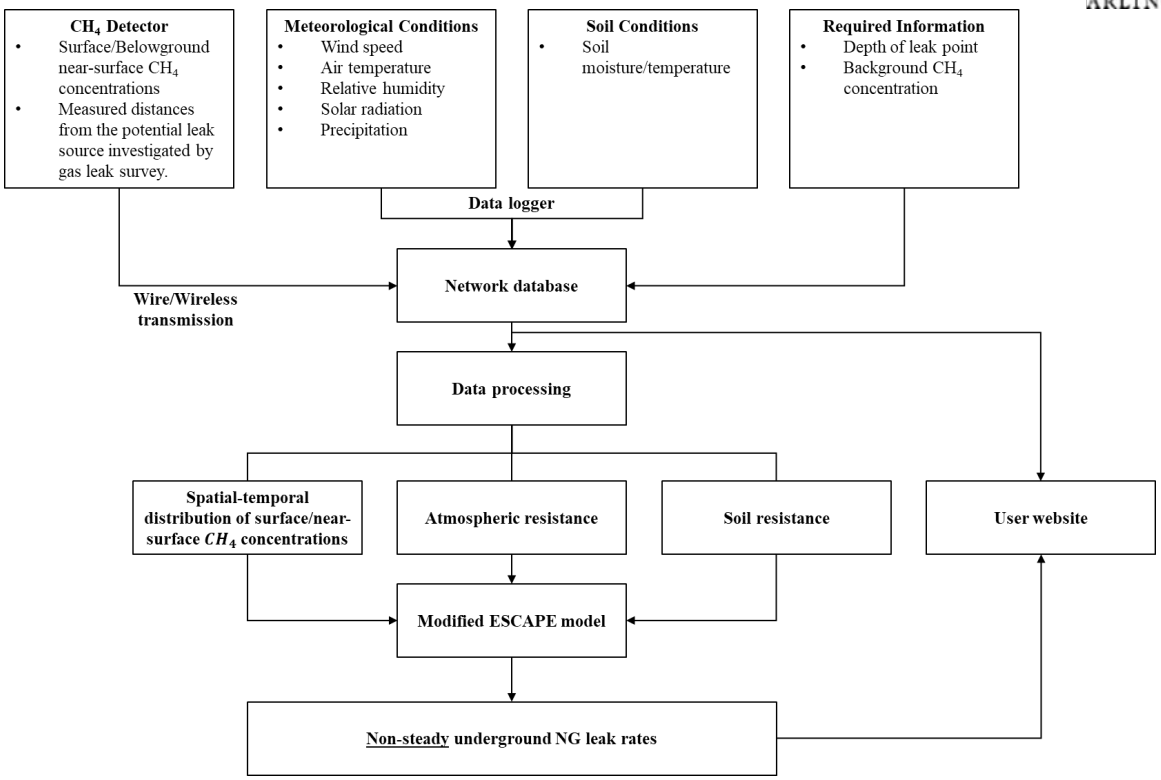

Figure 1. Conceptual framework of low-cost, near real-time CH_4 detector network. Required measurements include surface/near-surface CH_4 concentrations, meteorological conditions, soil conditions, depth of leak point, and the background CH_4 concentration. The measurements from CH_4 detectors could be transmitted wire and wirelessly through WiFi to the network database. Measured CH_4 concentrations were used to estimate the spatial-temporal distribution of surface and belowground near-surface CH_4 concentrations. Meteorological data and soil conditions were used to calculate the atmospheric resistance and the soil resistance. Estimated parameters are used in the modified ESCAPE model to estimate the non-steady belowground NG leak rates. The collected data and simulated results from the modified ESCAPE model are uploaded to the user website.

Low-cost Near Real-time CH_4 Detector

The low-cost, near real-time CH_4 detector, has been modified based on a previous low-cost CH_4 sensor design [Cho et al., 2022] to incorporate several enhancements. These enhancements include the capability to measure both surface and subsurface CH_4 concentrations, the integration of built-in connectivity options for wireless data transmission, and an expanded memory capacity for data storage.

The low-cost, near real-time CH_4 detector, consists of two metal oxide semiconductor (MOS) sensors (TGS2611-E00, Figaro USA Inc.), an environmental condition sensor (BME280, Bosch Sensortec Inc.), and a 16-bit analog-to-digital converter (ADS-1115) in a plastic case. The height, width, and length of the plastic case are 83.61 mm, 158.75 mm, and 177.7 mm, respectively (Figure 2). The MOS sensor is used to detect CH_4 concentrations due to its low cost, relatively high accuracy, and suitability for measuring CH_4 concentration levels in the atmosphere. The MOS has an optimal detection range of 500 to 12500 ppmv. The environmental condition sensor (BME280, Bosch Sensortec

Inc.) was used to monitor relative humidity with an accuracy of ± 3% and atmospheric temperature with a range from -40 to 85 ℃. Cho et al. (2022) suggested an approach to incorporate signals from the MOS sensor, atmospheric temperature, and relative humidity to estimate the CH_4 concentrations. Measured data is collected by a microcontroller, Raspberry Pi, with a microSD card in the detector at the frequency of 1 Hz. Two open tubes at the bottom of detectors (long and short) allow the surface and belowground near-surface CH_4 to meet MOS sensors. The depth of belowground near-surface CH_4 measurement is 1.2 cm (0.47 inches). The tube length on the CH_4 detector can be changed to measure at different depths as needed. In the soil and grass area, the shorter tube is placed flush on the soil surface while the longer tube penetrates 1.2 cm (0.47 in) below the ground surface. In the area with the impermeable surface cover (e.g., the asphalt), the two short tubes are used to monitor surface CH_4 concentration on the asphalt surface because we cannot dig a hole in the asphalt to bury the long tube (Figure 3).

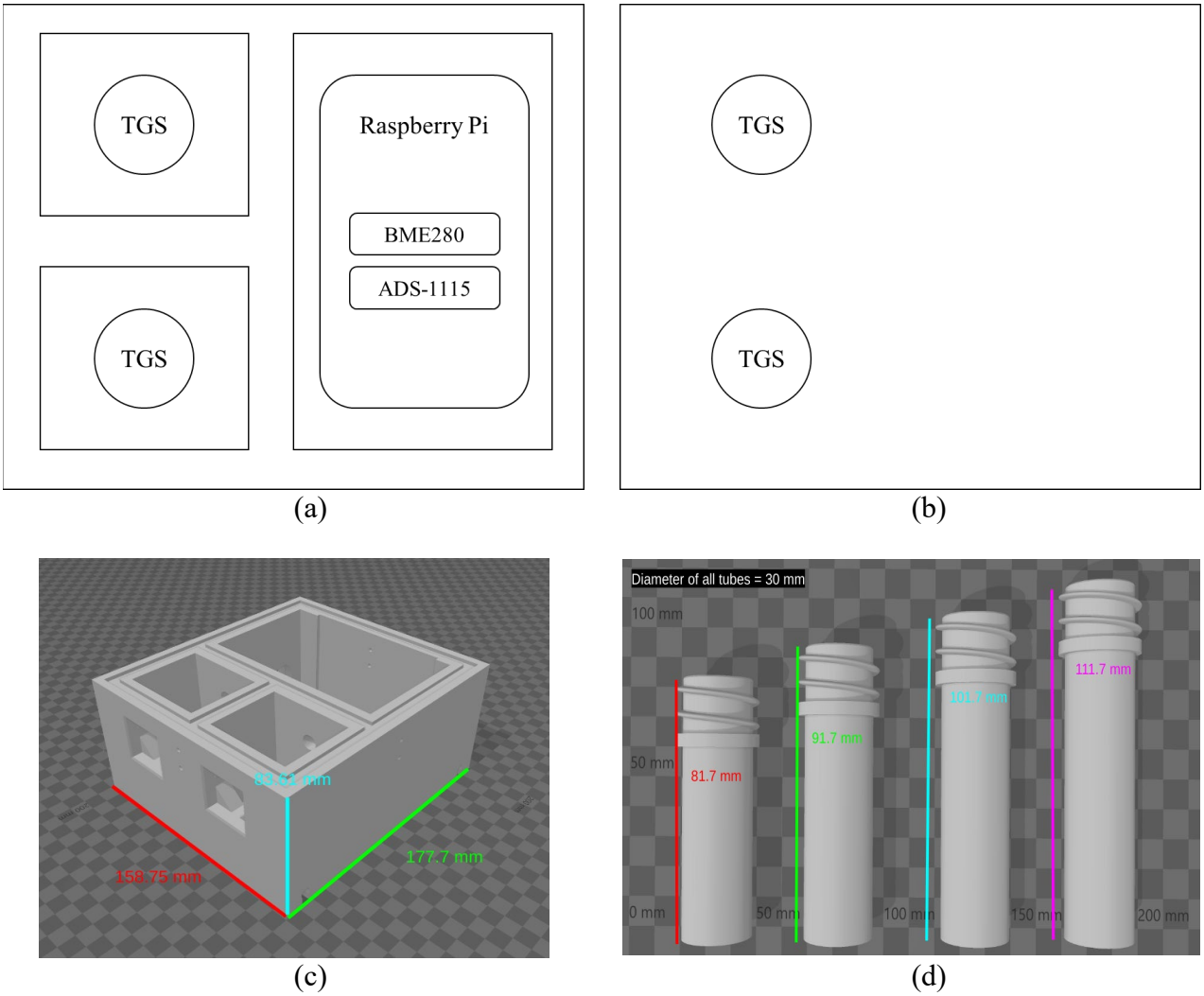

Figure 2. (a) Top view and (b) bottom view of the CH_4 detector. In the top view, the upper left CH_4 concentration sensor (TGS 2611-E, Figaro USA Inc.) is used to measure the surface CH_4 concentration, while the bottom left is used to measure belowground near-surface (BNS) CH_4 concentration (1.2 cm below the groundwater surface). The BME280 sensor is utilized to monitor air temperature, relative

humidity, and atmospheric pressure. The ADS-1115 is used to convert the measured signal from CH_4 concentration sensors. In the bottom view, the two holes at the bottom of the detector are connected to the opened tubes. (c) The size of the plastic case of the detector. (d) The lengths of opened tubes, which are used to measure CH_4 concentrations in different scenarios.

(a) (b)

Figure 3. Side views of the natural gas detector on (a) the asphalt area and (b) the soil and grass area. The detector on the asphalt area has two short open tubes of the same lengths. Both tubes connect to natural gas sensor (TGS) to measure surface methane concentrations. (b) The detector on the soil and grass area with one long and one short open tube. The short tube is responsible for measuring the surface methane concentration, while the long tube is responsible for monitoring the near-surface methane concentration at the depth of 0.12 cm below the ground surface.

Meteorological conditions

To measure the weather parameters needed for the model, a weather station (ATMOS 41, METER Group, Inc.) was utilized to monitor the changes in precipitation, solar radiation, relative humidity, atmospheric temperature, atmospheric pressure, and wind velocity. Measured meteorological data were used to estimate the atmospheric resistance in the modified ESCAPE model. The atmospheric resistance describes the influence of the quasi-laminar sub-layer of vegetation and the atmospheric stability on the gas migration between the surface and the atmosphere. Details of the estimation of atmospheric resistance can be found in Deliverable 3. Measurements from ATMOS 41 were recorded by ZL6 data loggers (METER Group, Inc.) at 30-second intervals.

Soil moisture and temperature

The soil moisture and temperature sensor (5TM, METER Group, Inc.) was used to monitor soil moisture and temperature at a depth of 10 cm below the ground surface at the leak site. Measured soil moisture and temperature were used to estimate the average soil resistance at a depth of 10 cm below the ground surface in the modified ESCAPE model. Soil resistance describes the influence of soil moisture on the belowground gas migration. Details of the estimation of soil resistance can be found in Deliverable 3. Measurements from 5TM were recorded by ZL6 data loggers (METER Group, Inc.) at 30-second intervals.

Near-real-time data collection and transmission

The collected data was uploaded to the network database and can be queried on the internal user

website. Measured surface and belowground near-surface CH_4 concentration from low-cost near real-time CH_4 detectors, atmospheric conditions (e.g., air temperature, precipitation, atmospheric pressure, and relative humidity) from the ATMOS 41 sensor, and soil conditions (e.g., soil moisture and temperature) from 5TM sensors during a specified period could be queried on the internal user website. The time scale of the performed data on the website is one change per 5 seconds. The node ID, which indicates the number of CH_4 detectors, measured parameters, and the time of measurement could be selected on the website (Figure 4). The measured parameters include air temperature, humidity, the voltage from the TGS sensor, and CH_4 concentration, which is estimated by the voltage [Cho et al., 2022]. The queried data could be output from the website in a .csv file and a .xlsx file.

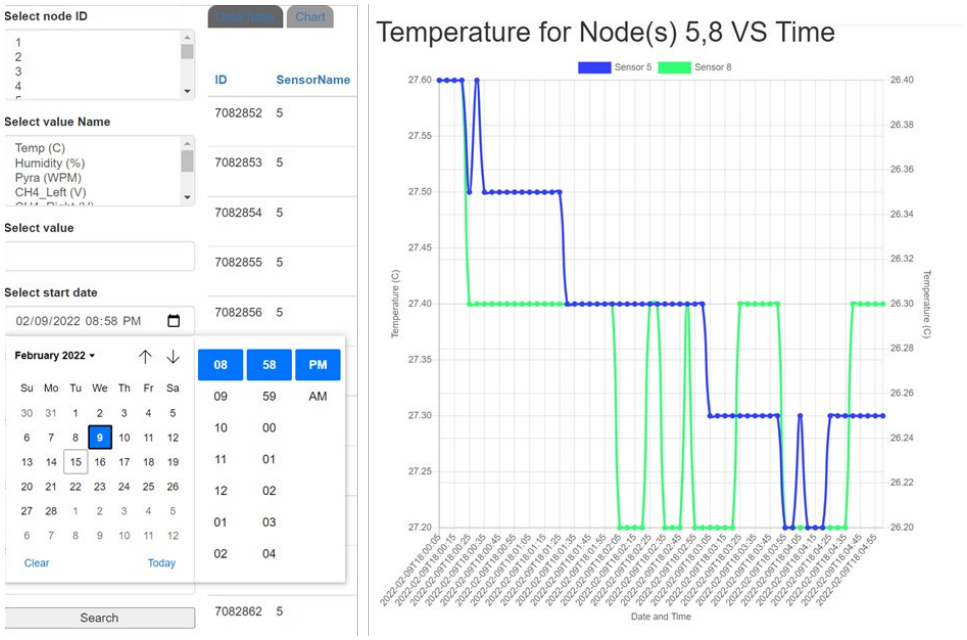

(a)

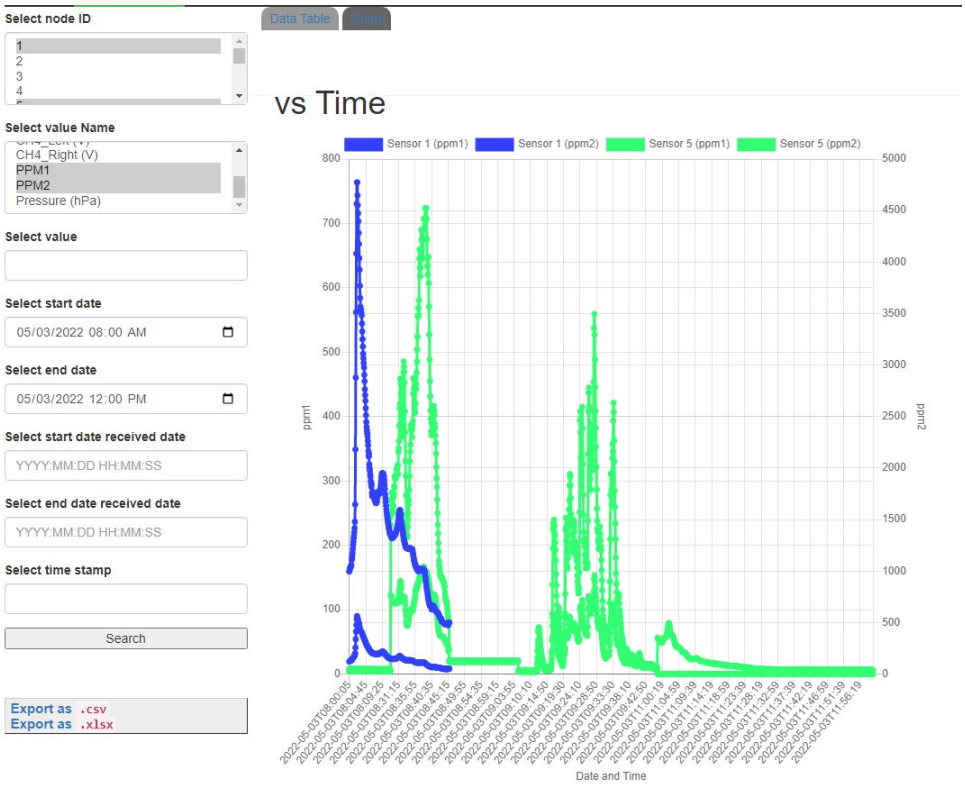

(b)

Figure 4. The screen shots from the user website. (a) The variations of measured air temperature by Nodes (Detector) 5 and 8. (b) The change in measured surface (ppm1) and belowground near-surface (ppm2) CH_4 concentrations. CH_4_Left and PPM1 indicate the surface measurements from the TGS sensor in the upper left of the detector, while CH_4_Right and PPM2 present the belowground near-surface measurement from the TGS sensor in the bottom left of the detector.

Calibration Tests of Natural Gas Detectors

The in-door and the field detector calibration tests with a commercially available trace gas analyzer (G4302 GasScouter, Picarro, Inc.) were conducted to calibrate MOS sensors in each detector. The in-door calibrations were conducted at an average ambient temperature of 19℃ and 37% averaged relative humidity. The inlet tube of the trace gas analyzer (G4302 GasScouter, Picarro, Inc.) was positioned at an identical elevation as the bottom of the detector tube to ensure CH_4 measurements were taken at the same height during the calibration process. The details of the calibrations of the MOS detectors can be found in Cho et al. (2022). CH_4 gas with a purity of 99.99% is directly released from the gas cylinder by a pressure regulator at a pressure of 1-1.5 (psi) for 20 minutes. After 20 minutes, we turned off the methane gas and waited 15 mins until the methane concentration decreased to the background concentration (2 to 3 ppmv). In the field calibration, the MOS sensors and the trace gas analyzer (G4302 GasScouter, Picarro, Inc.) monitored the variation of CH_4 at 12 cm above the ground surface for 40 minutes with a constant gas leak rate of 10.8 SCFH.

The correlations between two MOS sensors in each detector were generally greater than 0.7

(R^2>0.7) at the gas concentration between 500 to 1500 ppmv (Figure 5). Some measured CH_4 concentrations from Picarro G4302 fluctuated more than results from natural gas detectors (Figure 6). It could be due to the sudden changes in methane concentration which saturated the chamber in the Pircarro G4302 and slowed down the measurement frequency of the Picarro G4302. Furthermore, the released methane gas was controlled by a pressure regulator. To keep the constant gas pressure, the release rate of methane changed during the test and thus induced the fluctuation in measurements of methane concentration. In the field calibration test, the trend of measured methane concentration from the Picarro G4302 was similar to the change of methane concentration from two TGS sensors in Detectors 14 and 16 (Figure 7).

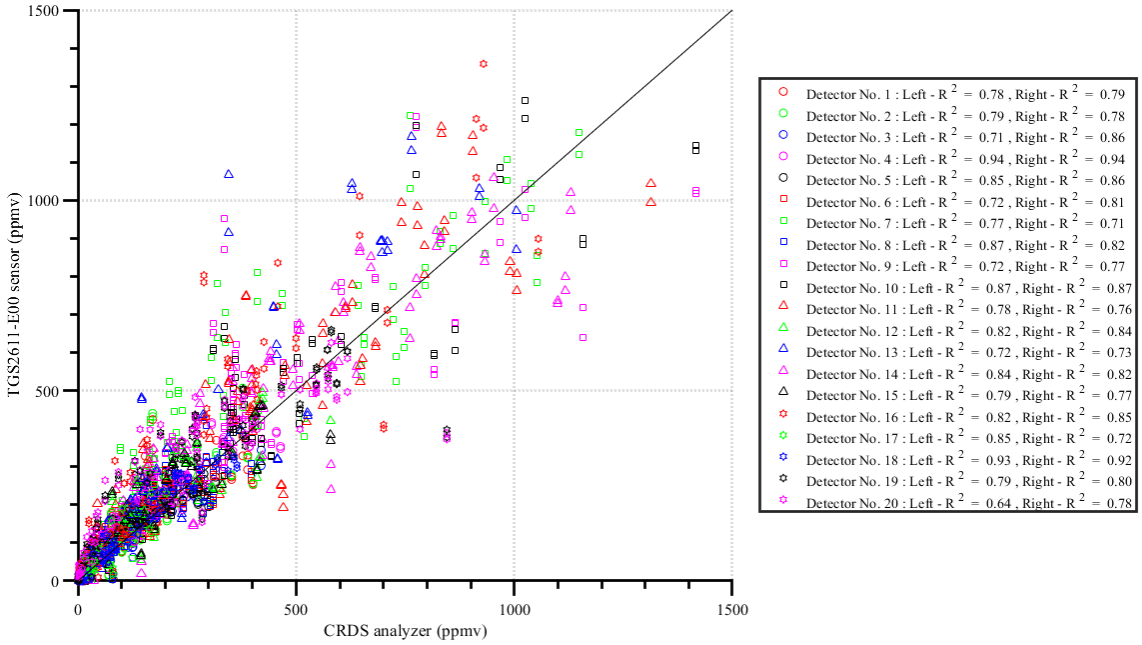

Figure 5. The correlation between two TGS sensors (left and right) in the CH_4 detector. The Left-R^2 shows the correlation coefficient between the bottom left TGS sensor in the detector and the trace gas analyzer (Picarro G4302). The Right-R^2 shows the correlation coefficient between the upper left TGS sensor in the detector and the trace gas analyzer (Picarro G4302).

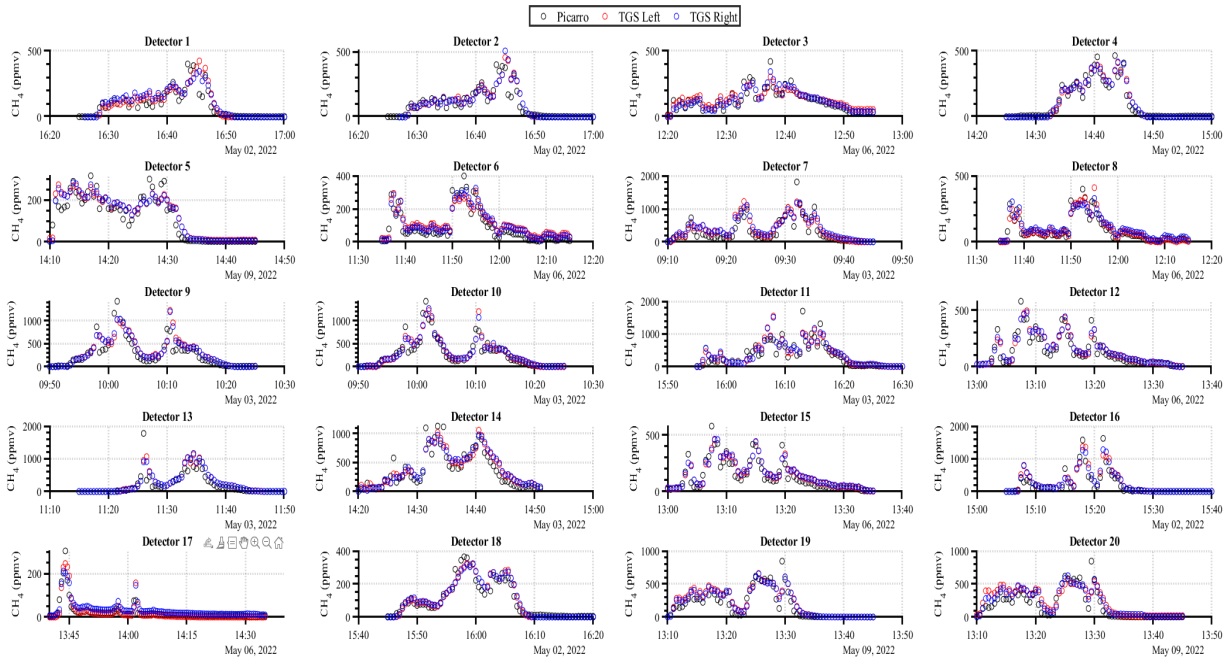

Figure 6. Measured CH_4 concentrations by trace gas analyzer (Picarro G4302) and CH_4 detectors in the in-door calibration. The black point indicates the measurement from the trace gas analyzer (Picarro G4302). The blue point presents measurements from the upper left TGS sensor in the detector, while the red point shows measurements from the bottom left TGS sensor in the detector. The data from CH_4 detectors and CRDS were averaged at 100-second intervals.

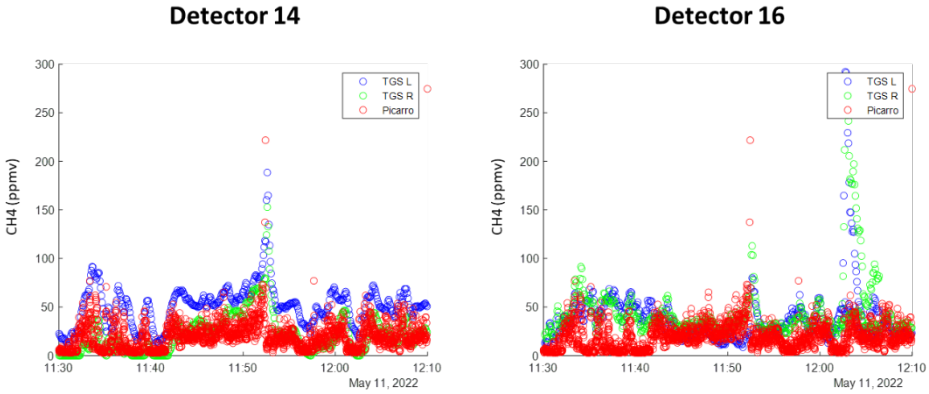

Figure 7. Measured CH_4 concentrations by trace gas analyzer (Picarro G4302) and CH_4 detectors in the field calibration. The red point indicates the measurement from the trace gas analyzer (Picarro G4302). The blue point presents measurements from the bottom left TGS sensor in the detector, while the green point shows measurements from the upper left TGS sensor in the detector. The data from CH_4 detectors and CRDS were averaged at 100-second intervals.

Key Findings

- The low-cost, near real-time methane (CH_4) detector was modified based on a prior design of a low-cost CH_4 sensor [Cho et al., 2022], enhancing the ability to measure both surface and subsurface CH_4 concentrations, integration of built-in connectivity options for wireless data transmission, and an expanded memory capacity to increase data storage requirements.
- A comparison of the low-cost, near real-time CH_4 detector and a commercially available trace gas analyzer (G4302 GasScouter, Picarro, Inc.) was in good agreement, demonstrating the effectiveness of a universal calibration model developed in this study which accounts for sensor-specific variation for measurements of CH_4 concentrations. In field experiments, the low-cost, near real-time CH_4 sensor measured CH_4 concentrations reliably enough to detect changes in the emission state of an underground pipeline leak.
- A comparative analysis between the low-cost, near real-time CH_4 detector and a commercially available trace gas analyzer (G4302 GasScouter, Picarro, Inc.) revealed a good agreement, highlighting the effectiveness of a universal calibration model developed in this study. The calibration model accounts for sensor-specific variations in measuring CH_4 concentrations.
- The internal user website was developed to collect near-real-time measurements of surface and belowground near-surface CH_4 concentrations, along with environmental conditions such as temperature, relative humidity, and air pressure, from the low-cost, near-real-time CH_4 detector. This website allows industry professionals and end-users to easily query and visualize the collected data, providing a quick understanding of the current situation regarding surface and belowground CH_4 emissions and environmental conditions in the field. It serves as a user-friendly platform for monitoring and assessing the dynamic nature of CH_4 emissions and related environmental factors.

Deliverable 2: Comprehensive Experimental Data Sets from METEC Test Site

Objective

- A series of controlled field-scale experiments are conducted at the METEC site at CSU to evaluate the performance of the low-cost, near real-time CH_4 detector network and simulation-optimization algorithm. These experiments cover a wide range of field conditions, including subsurface, surface, and atmospheric variables. The focus is to determine the optimal detector configuration for different rural and urban leakage scenarios and test the effectiveness of the detector network linked to the optimization-decision-making algorithm using near real-time data. These experiments also provide valuable insights for improving leak detection, monitoring, and response strategies, enhancing methane emission management.

Experimental Site

To evaluate the performance of the low-cost near-real-time CH_4 detector network and the simulation-optimization algorithm, we performed a series of controlled field-scale experiments at the Methane Emission Technology Evaluation Center (METEC). A detailed description of the experimental testbeds can be found in Ulrich et al., (2019) and Gao et al., (2021). The METEC site was developedby CSU in response to the Department of Energy (DOE)'s call for a testing facility and proving ground for ARPA-E Methane Observation Networks with Innovative Technology to Obtain Reductions (MONITOR). The 7-acre test facility includes well pads, small compressor stations, and underground pipelines. The design focuses on recreating realistic site configurations to simulate dispersion. In total, there are 198 aboveground and 52 belowground release points with 60 of these points being able to be controlled simultaneously. METEC is seen as a key facility by operators and environmental groups for continued study and research in the oil and gas field. Figure 8 shows an aerial view of the site with the pipeline test bed location.

Specific to this project, METEC includes a unique underground pipeline testbed that allows for the simulation of underground pipeline leaks at known leakage rates in varying subsurface (e.g., soil type, texture, moisture) and surface (e.g. precipitation, pavement, vegetation) conditions. This site provides a unique ability to both control and measure subsurface and surface conditions on a continuous basis and provides a wide range of testing conditions. For example, we can spatially and temporally measure the gas concentration throughout the soil domain, allowing us to determine the gas migration patterns with time, thus providing an ideal location to evaluate gas migration sensitivities and develop recommended practices for subsurface gas migration mitigation.

- We performed a series of field-scale controlled NG release experiments at the METEC test site to evaluate the performance of the low-cost near-real-time CH_4 detector network and the simulation optimization algorithm. The testbed was designed to simulate the transportation of natural gas from the pipeline in undisturbed soil and grass area without an impermeable surface cover [Ulrich et al., 2019]. Polyvinyl chloride (PVC) pipe at a depth of 0.91 m below the ground surface (BGS), simulated a leaking pipeline at a depth consistent with the natural soil cover requirements for buried pipelines. The size and depth of the buried pipelines were selected to represent those of typical NG distribution mains.

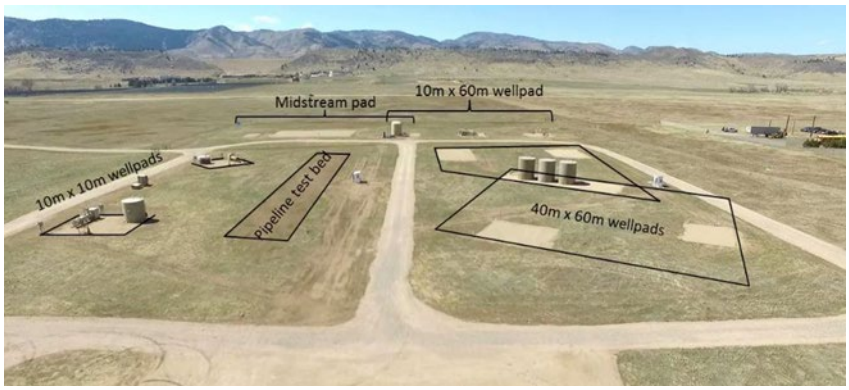

Figure 8. METEC Test Facility. Additional details on the overall site can be found at - https://energy.colostate.edu/areas-of-expertise/methane/metec-at-colorado-state-university/

Summary of Experiments

As seen in Table 1, a 7-day controlled experiment was conducted at the METEC site. Experiments varied in terms of leakage rate (22.6 ± 5.5g CH_4 $h^{-1}$to 369.5 g CH_4 h^{-1}), soil conditions (homogenous soil, moisture, and soil temperature), and weather conditions. Each experiment will be outlined in the following sections, but a summary of the experiments is provided here.

Table 1. Overview of tests, calibration, and field experiments of the natural gas (NG) detector.

Exp. Type	Exp. Number	Averaged Flow Rate (g CH_4 hr^{-1})	Duration	Testbed	Steady State(SS)/ Transient(T)	Surface Condition
Surface	#1	22.6 ± 5.5*	120 hours	Rural	SS	Open
Surface	#2	84.4 ± 9.7*	120 hours	Rural	SS	Open
Surface & Subsurface	#3	37 ± 4.8*	48 hours	Rural	T	Open
		89 ± 6.8*	36 hours	Rural	T	Open
		121 ± 4.4*	36 hours	Rural	T	Open
		190 ± 25.4*	48 hours	Rural	T	Open
Surface & Subsurface	#4	18.5	24 hours	Urban	T	Partial Coverage
		184.6	24 hours	Urban	T	Partial Coverage
		369.5	72 hours	Urban	T	Partial Coverage

*Mean emission rate with one standard deviation set for the controlled experiments

Experiment #1 & #2

Experiments #1 and #2 were conducted at the rural testbed located at METEC for a duration of 5 days each. The leak rates in Experiment #1 were recorded as 22.6 ± 5.5 g CH_4 h^{-1}, while in Experiment #2, the leak rates were measured as 84.4 ± 9.7 g CH_4 h^{-1}. For a comprehensive understanding of the testbed setup, a detailed description can be found in Ulrich et al. (2019) and Cho et al. (2020). Furthermore, the testbed consists of stainless-steel tubing and a 10 cm diameter polyvinyl chloride

(PVC) pipe, both buried at a depth of 0.9 m underground. Compressed natural gas, consisting of 86% CH_4, is delivered through the stainless-steel tubing at a specified rate and location to simulate gas release. Figure 9 illustrates the deployment of CH_4 detectors in both Experiments #1 and #2. The adjacent PVC pipe represents a leaking pipeline.

At METEC, surface CH_4 concentrations were continuously monitored using 19 NG detectors, which were positioned directly on the soil surface of the testbed. Each CH_4 detector consists of a microcontroller, a natural gas sensor (TGS2611-E00, Figaro USA Inc.), a temperature/relative humidity sensor (SHT35-DIS-F2.5KS digital sensor, Sensirion AG), and a piezoresistive absolute pressure sensor (LPS25HB, STMicroelectronics). The SHT35-DIS-F2.5KS sensor exhibits an accuracy of ±0.1 °C and ±1.5% relative humidity (RH). Atmospheric pressure was measured using a piezoresistive absolute pressure sensor (LPS25HB, STMicroelectronics) with an accuracy of ±0.01 psi. The CH_4 detectors received electrical power through a power over ethernet (PoE) switch connected via ethernet cables. Data was collected by the CH_4 detector at a frequency of 1 Hz using the microcontroller. Prior to the experiments, all sensors were calibrated following the recommended approach by Cho et al. (2022).

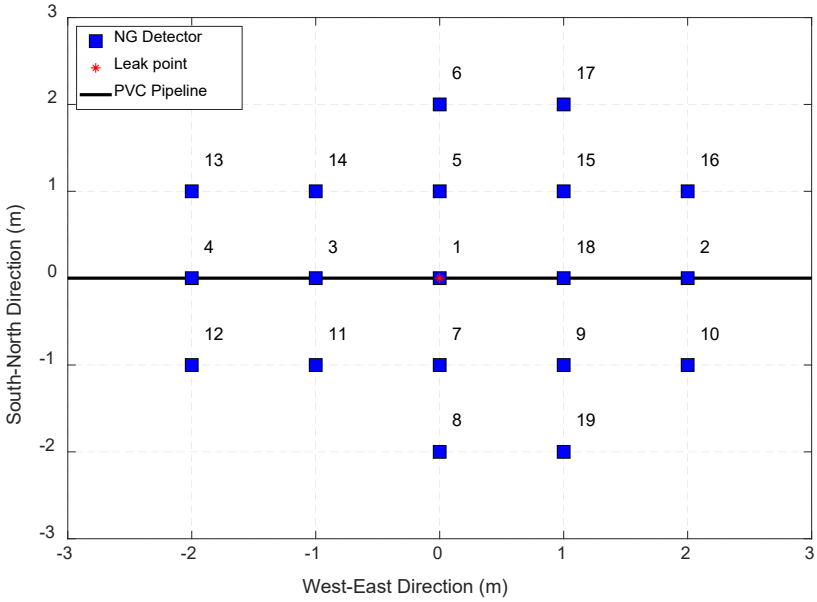

Figure 9. A top view of sensor layout on a testbed at the METEC site. A pipeline runs east to west, which is buried 0.91 m belowground, and the underground controlled release of NG is located at the center (Detector 10). 19 NG detectors were placed on the ground.

Surface CH_4 Concentrations

The measured surface CH_4 concentrations during the experiment are shown in Figure 10. The diurnal cycle of surface methane concentration was consistently observed under constant leak rates from the two controlled gas release experiments. During the daytime, the methane concentration typically drops and then rises at night. The ratio of average methane concentration observed during night and day varied from 1.1 to 1.8. As air temperature decreased, surface methane concentrations tended to increase. This can be attributed to the influence of temperature on gas dispersion and changes in density result in significant variations in methane concentration. Ground heat fluxes cause gas molecules to spread apart slightly, occupying a larger volume and leading to a decrease in density. Additionally, rising surface temperatures promote atmospheric turbulence, facilitating the dispersal of

methane.

Figure 11 shows the top-view of the spatial distribution of CH_4 plumes measured on the surface when the averaged leak rate was increased from 22.5 (g CH_4 hr^{-1}) to 84.4 (g CH_4 hr^{-1}). With the elevation in the controlled gas leak rate, the overall surface CH_4 concentration increased. For example, the surface CH_4 concentration at the center (0 m) increased by approximately 70% from 357 ppmv to 604 ppmv as the controlled gas leak rate increased from 22.5 to 84.4 (g CH_4 hr^{-1}). The surface CH_4 concentrations decreased from the center (0 m) to the boundary of the testbed. Furthermore, the surface CH_4 plumes extended from the leak point to the boundary of the testbed. The plume area of the surface CH_4 at the average leak rate of 22.5 (g CH_4 hr^{-1}) extended approximately 1.25 times farther than that of the surface CH_4 at the average leak rate of 84.4 (g CH_4 hr^{-1}). These results indicate that the low-cost, near real-time CH_4, could capture the variation of surface CH_4 concentrations at a constant gas leak rate scenario.

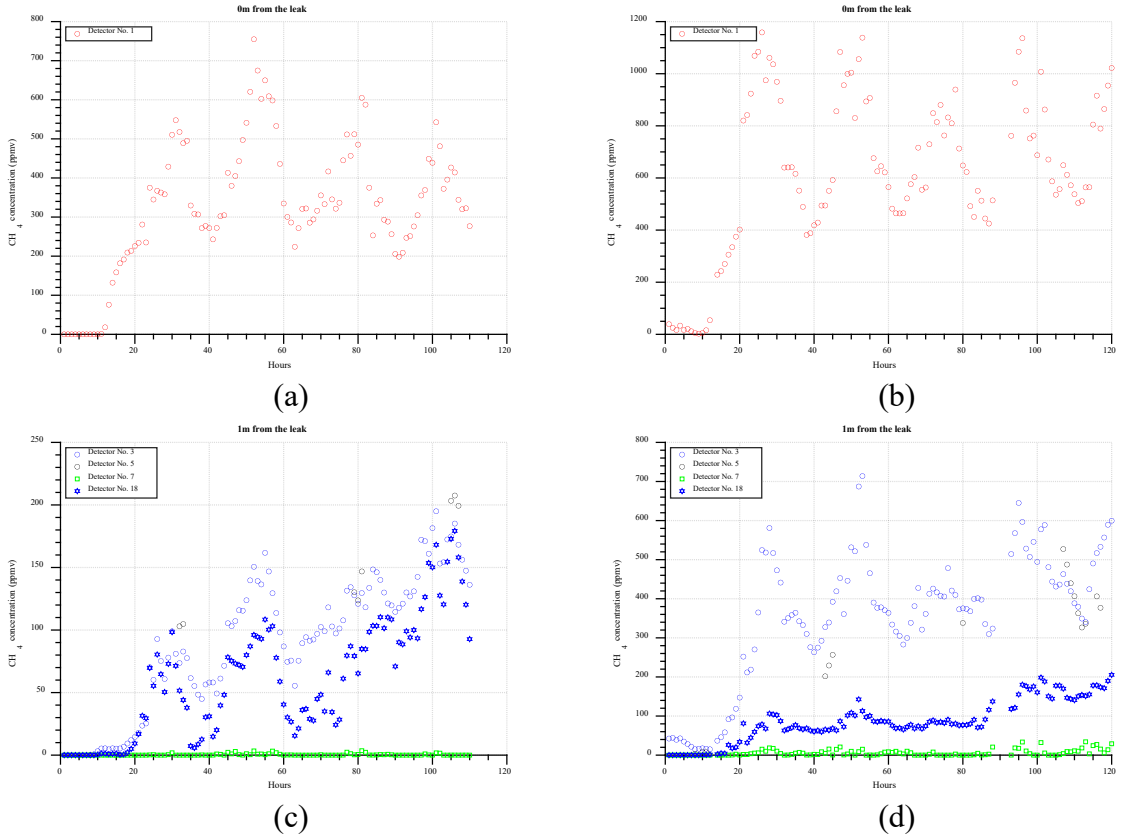

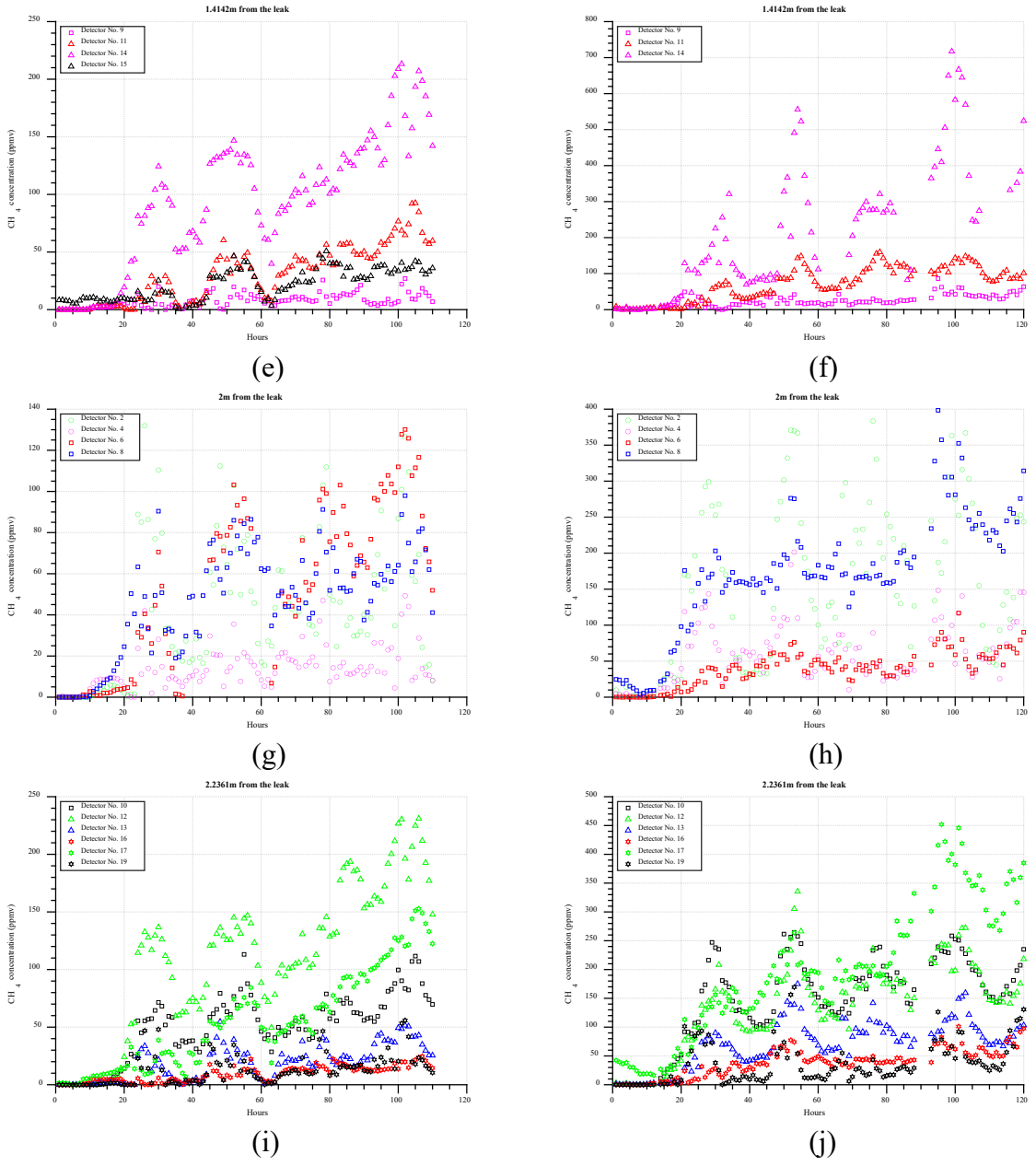

Figure 10. Measurements of surface CH_4 concentrations at (a) 0, (c) 1, (e) 1.4, (g) 2, and (i) 2.2 m from the leak point at the NG release rates of 22.5 ± 5.5 g CH_4 hr^{-1}, and at (b) 0, (d) 1, (f) 1.4, (h) 2, and (j) 2.2 m from the leak point at the NG release rates of 84.4 ± 9.7 g CH_4 hr^{-1}.

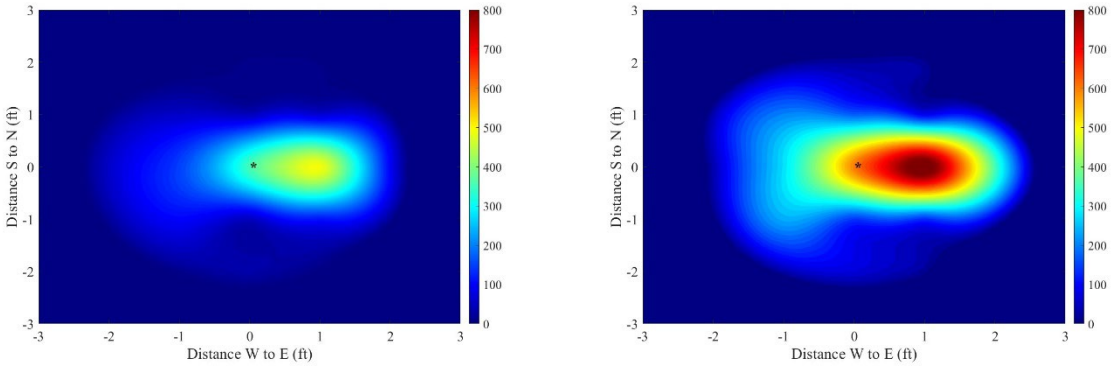

(a) (b)

Figure 11. Top view of observed spatial distribution of surface and CH_4 expression (ppmv) at the NG release rates of (a) 22.5 ± 5.5 (g CH_4 hr^{-1}) and (b) 84.4 ± 9.7 (g CH_4 hr^{-1}). The star maker (*) in the contour presents the location of the leak point.

Experiment #3

In Experiment #3, surface and belowground near-surface (1.2 cm below the ground surface) CH_4 concentrations were measured over time using 19 CH_4 detectors which were placed directly on the soil/grass area at the testbed (Figure 13). Each CH_4 detector was assembled with two natural gas sensors (TGS2611-E00, Figaro USA Inc.), an environmental sensor (BME280, Adafruit), and a wireless transmitter on the microcontroller. Two open-ended tubes at the bottom of the CH_4 detector provide a path to individual CH_4 sensors. Two different tube lengths were used for surface and belowground near-surface CH_4 measurements. The tube length on the CH_4 detector can be changed to measure at different depths as needed (Figure 2d). A power over ethernet (PoE) switch with network cables was used to carry electrical power to each CH_4 detector. The CH_4 detector collected the data at 1 Hz in the microcontroller. The meteorological data were collected by an on-site weather sensor above the ground surface at 50 cm. Experiments varied in terms of their leak rates and environmental conditions in 7 days. The range of leak rates was from 37 ± 4.8 g CH_4 hr^{-1} to 190 ± 25.4 g CH_4 hr^{-1} (Table 1). Changes in the soil moisture content were continuously monitored by 5TM (METER Group, Inc.). The leak rates during the experiment were increased stepwise over 7 days to understand the changes in response to the low-cost near real-time CH_4 detector network. A detailed description of a testbed can be found in Ulrich et al. (2019) and Cho et al., (2020).

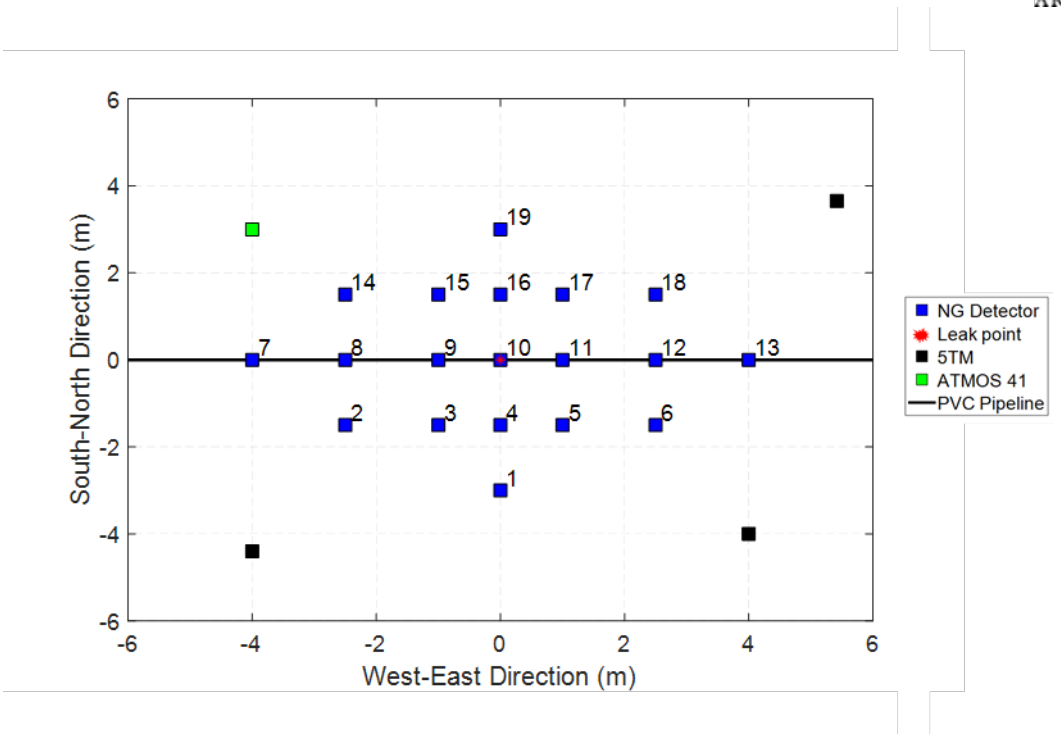

Figure 12. A top view of sensor layout on a testbed at the METEC site. A pipeline runs east to west, which is buried 0.91 m belowground, and the underground controlled release of NG is located at the center (Detector 10). Blue squares indicate CH_4 detectors on the ground. Black squares present three soil moisture sensors (5TM) that were buried at 0.10 m below the ground surface. The green square shows the on-site weather sensor (ATMOS 41).

Surface and Belowground Near-surface CH_4 Concentrations and Plumes

The measured surface and belowground near-surface (BNS) CH_4 concentrations showed increasing trends with the increase of controlled gas leak rates (Figure 13). With the increase of measured distance from 0 m to 4 m, the range of variation of measured surface and belowground near-surface CH_4 concentrations decreased. The decrease in the concentration indicated the extent of CH_4 migration from the center toward the testbed boundary. This gas migration is induced by advection and diffusion, which are induced by the difference of pressure on the surface and belowground near-surface. During the experiment, the highest averaged surface and BNS CH_4 concentrations were detected at the center (0 m), which was directly above the leak point, with 3497 ppmv and 4229 ppmv (Figure 13a). Experimental results indicate that elevated BNS gas concentrations persist long before elevated surface concentrations are observed. On average, BNS CH_4 concentrations (1.2 cm below the soil surface) were higher than average surface concentrations with the range from 20% to 486% within a monitoring radius of 4 meters. In addition, with an increase in the leak rate from 37 to 84 g/h, an increase in the BNS CH_4 concentration was observed within 3 hours with an increasing leak rate. However, the surface CH_4 concentration did not perform significant changes compared to the BNS CH_4. The slight change in the surface CH_4 concentration is induced by atmospheric variability (e.g., wind speed and temperature). The increases in air temperature could promote atmospheric turbulence, impeding the gas migration from the surface to the atmosphere. Furthermore, a comparison between surface CH_4 flux and the atmospheric resistance (R_{at}) indicates that the high atmospheric resistance could reduce

the transportation of CH_4 flux from the surface to the atmosphere. With the decrease in the soil moisture, the soil resistance increased and elevated the BNS CH_4 fluxes. Therefore, the overall BNS CH_4 concentration is higher than the overall surface CH_4 concentration.

Figure 15 shows the top-view of the spatial distribution of CH_4 plumes measured on the surface (Figure 15a, 15c, and 15e) and in BNS (Figure 15b, 15d, and 15f) when the averaged leak rate was increased from 88.76 (g CH_4 hr^{-1}) to 120.96 (g CH_4 hr^{-1}) between hour 84 and hour 86. The surface and BNS CH_4 concentrations decreased from the center (0 m) to the boundary of the testbed. Furthermore, the surface and BNS CH_4 plumes extended from the leak point to the boundary of the testbed. The plume area of the BNS CH_4 extended approximately two times farther than that of the surface CH_4 as the gas leak rate increased from 37 (g/h) to 121 (g/h). Due to atmospheric variability, any changes in surface CH_4 concentrations may not be readily apparent within this period. The slight variations in surface CH_4 concentrations can be influenced by meteorological conditions above the ground surface, such as wind speed and temperature. The increase in air temperature enhances the ground heat fluxes, causing turbulence to decrease the mass of gas on the surface. Furthermore, the substantial difference between surface and below-near-surface (BNS) methane concentrations and plumes indicates that surface methane expression may not fully represent the conditions of BNS methane expression. Hence, the measurement of BNS methane should be significantly considered when understanding the non-steady gas migration of methane from the subsurface to the atmosphere.

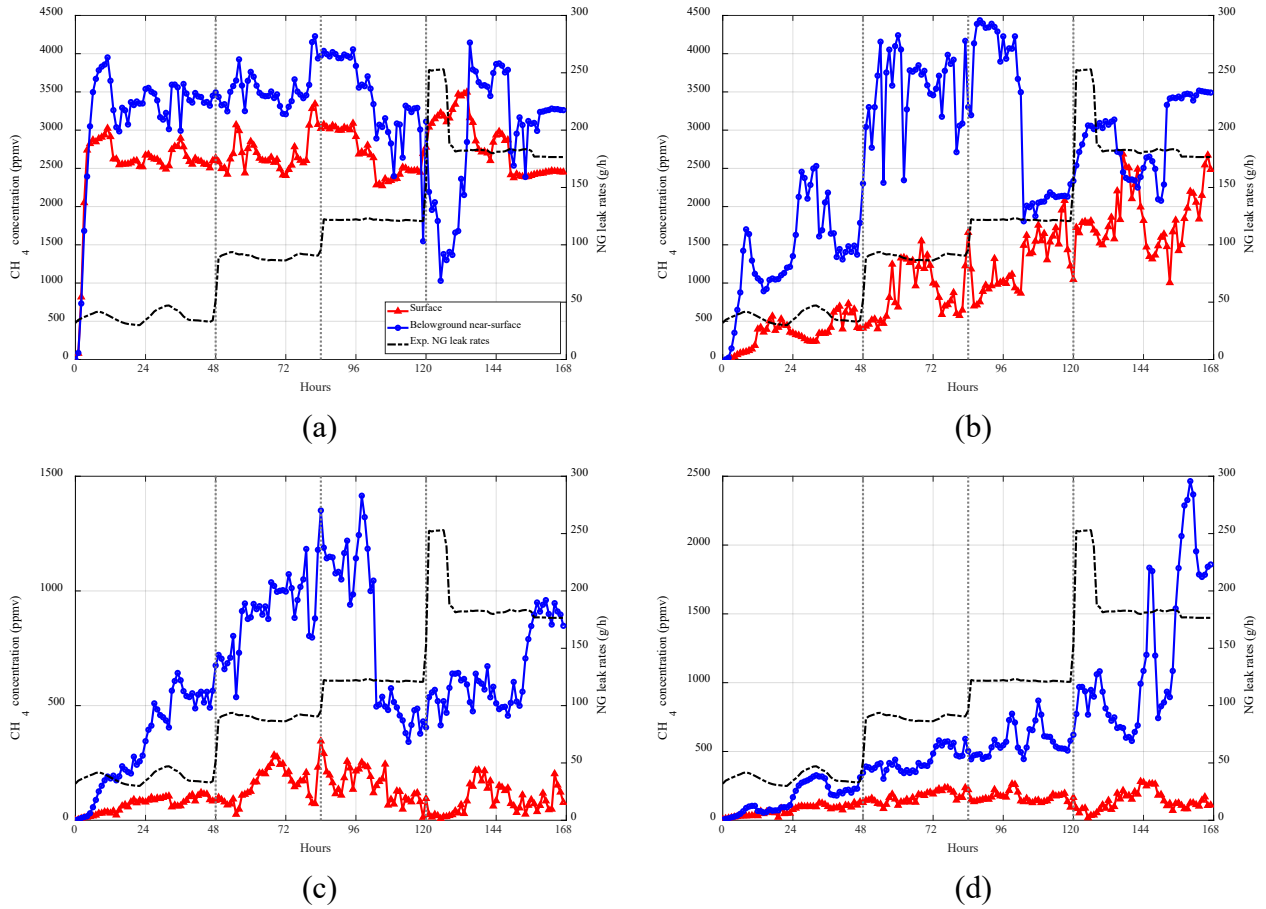

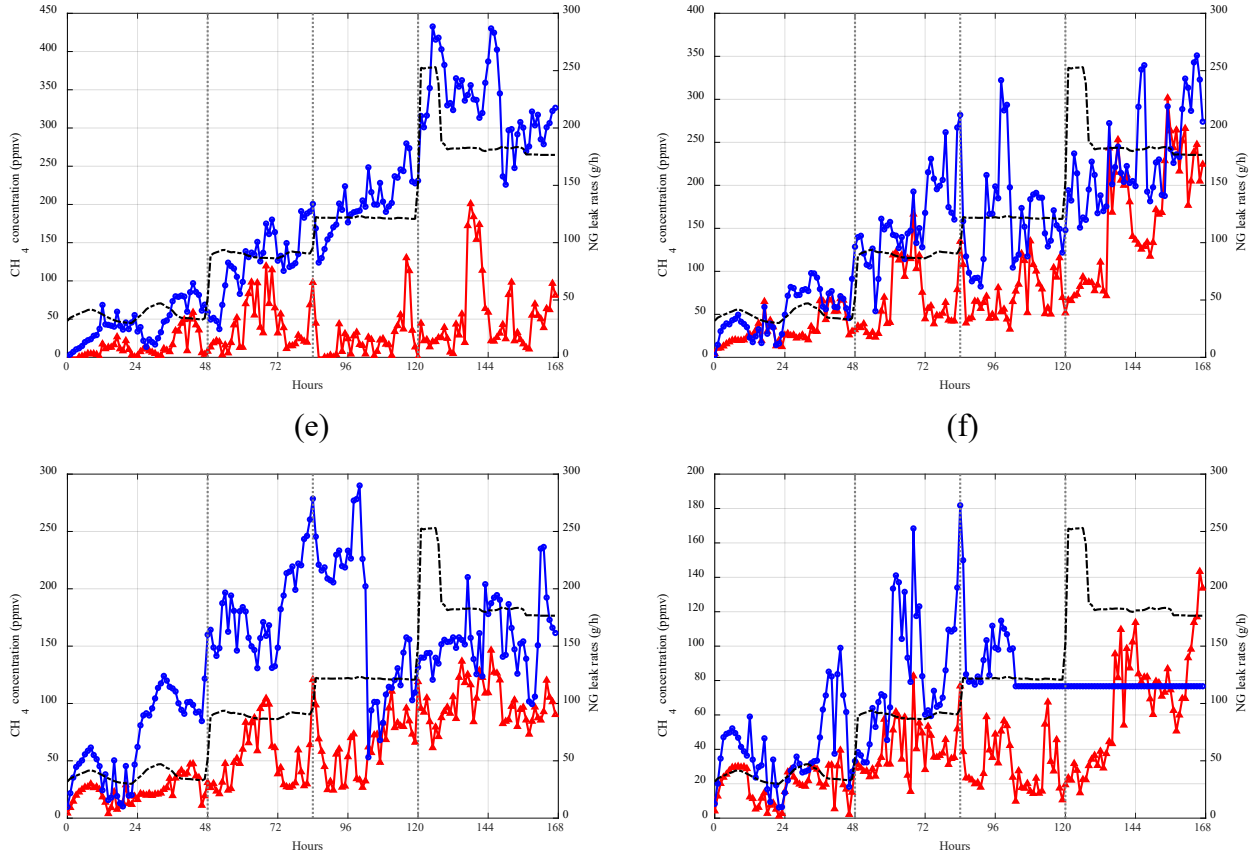

Figure 13. Measurements of maximum surface and BNS CH_4 concentrations at (a) 0, (b) 1, (c) 1.5, (d) 1.8, (e) 2.5, (f) 2.9, (g) 3, and (h) 4 m from the leak point. The red line presents subsurface methane concentration, while the blue line indicates BNS CH_4 concentrations. The dashed line presents the controlled NG leak rates (g CH_4 hr^{-1}). The gray dotted lines indicate the time when controlled NG release rates (g CH_4 hr^{-1}) were increased from 37.08 (g CH_4 hr^{-1}) to 88.76 (g CH_4 hr^{-1}) at hour 48, from 88.76 (g CH_4 hr^{-1}) to 120.96 (g CH_4 hr^{-1}) at hour 84, and from 120.96 (g CH_4 hr^{-1}) to 190.24 (g CH_4 hr^{-1}) at hour 84.

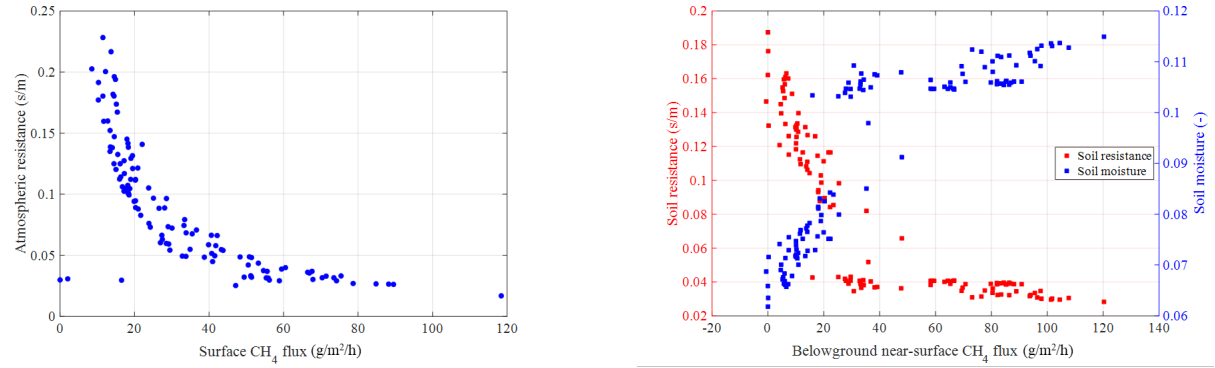

Figure 14. (a) Comparison of surface CH_4 fluxes ($g/m^2/h$) and atmospheric resistances (s/m). (b) Comparison of BNS CH_4 fluxes and soil moisture and soil resistance.

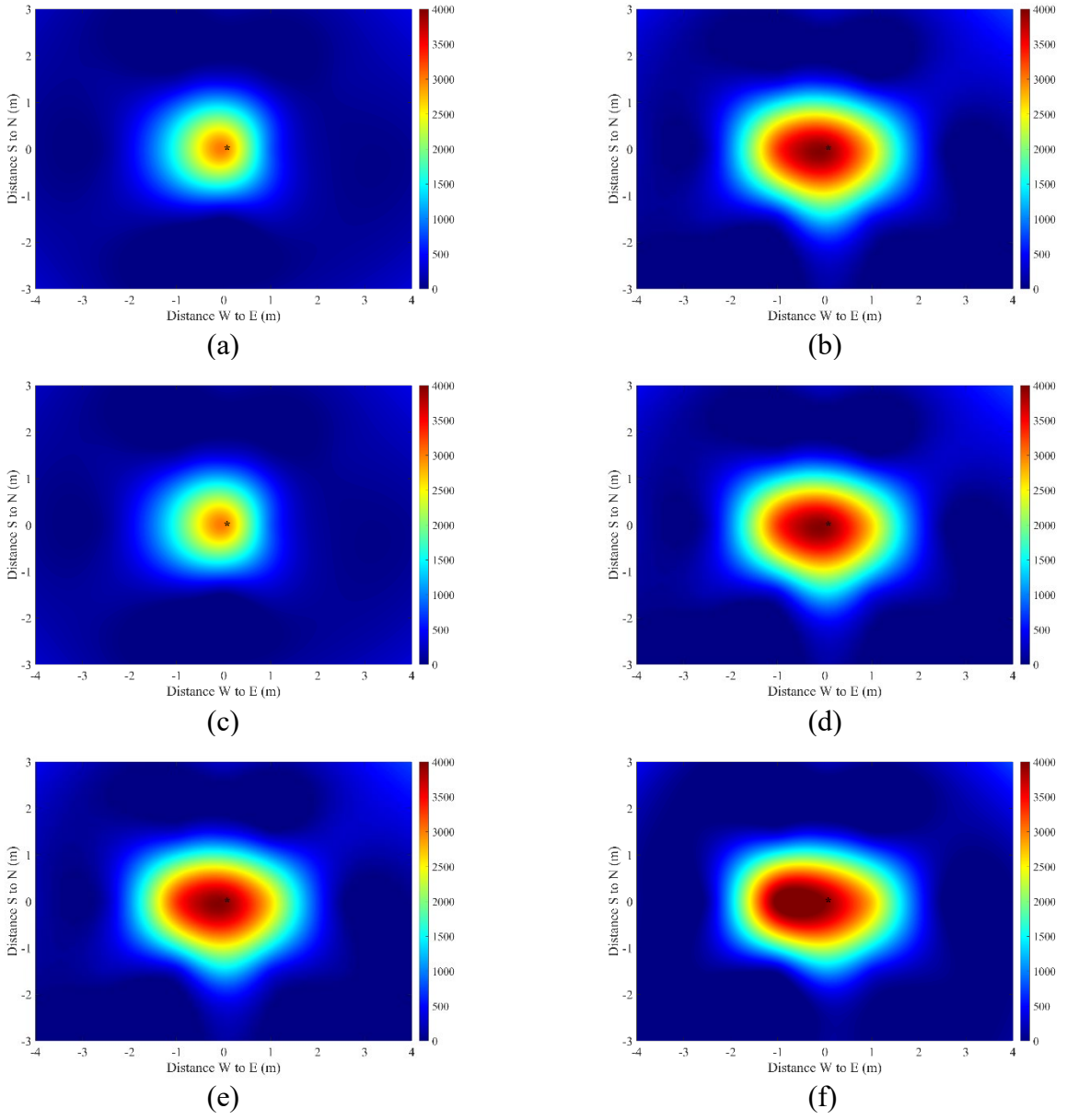

Figure 15. Top view of observed surface (a, c, and e) and BNS (b, d, and f) CH_4 expression (ppmv) from hour 84 to hour 86. The controlled gas leak rate increased from 88.76 (g CH_4 hr^{-1}) to 120.96 (g CH_4 hr^{-1}) during this period. The star maker (*) in the contour presents the location of the leak point.

Experiment #4

In Experiment #4, surface and belowground near-surface (1.2 cm below the ground surface) CH_4 concentrations in the scenario with the impermeable surface cover were measured over time using 9 CH_4 detectors (Figure 16). A CH_4 detector (Detector 4) was placed on the asphalt area, where was

directly above the leak point. Six CH_4 detectors were deployed around the edge of asphalt (Detectors 2, 7, 10, 11, 13, and 20). Three CH_4 detectors were set up on the grass/soil area (Detectors 6 and 12). Two open ended tubes installed at the bottom of the CH_4 detector provided a path to individual CH_4 sensors. Two different tube lengths were used for surface and belowground near-surface measurements on the soil/grass area and around the edge of the asphalt. A power over ethernet (PoE) switch with network cables was used to carry electrical power to each CH_4 detector. The CH_4 detector collected the data at 1 Hz in the microcontroller. The meteorological data were collected by an on-site weather sensor above the ground surface at 50 cm. Experiments varied in terms of their leak rates and environmental conditions in 5 days. The range of leak rates was from 18.5 g CH_4 hr^{-1} to 369.5 g CH_4 hr^{-1} (Table 1). Changes in the soil moisture content at 10 cm below the ground surface were continuously monitored by 5TM (METER Group, Inc.). The leak rates during the experiment were increased stepwise over 5 days to understand the changes in surface and BNS CH_4 concentrations with the impermeable surface cover to the low-cost near real-time CH_4 detector network.

Experimental measurements are still in the works of data processing. We will present the results and analysis in the final version of the report.

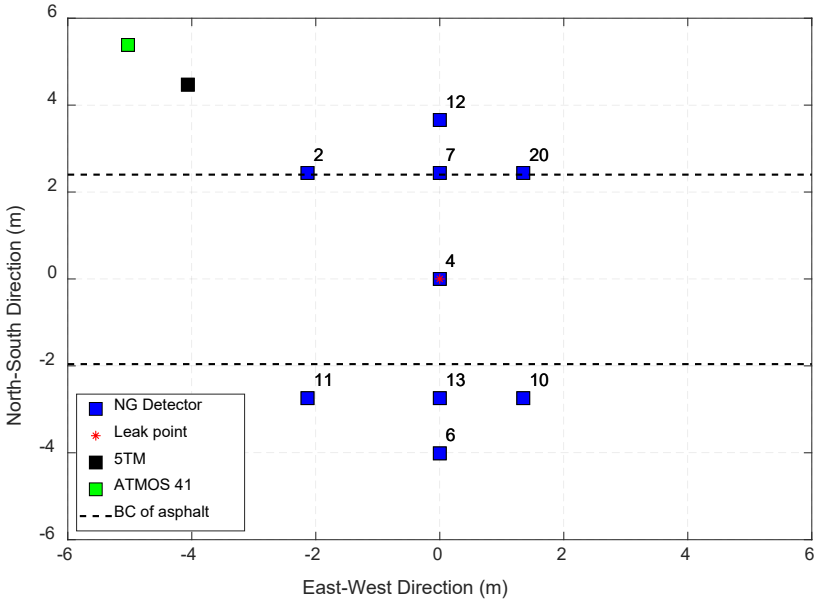

Figure 16. A top view of sensor layout on a testbed at the METEC site. A pipeline runs east to west, which is buried 0.91 m belowground, and the underground controlled release of NG is located at the center (Detector 10). 19 NG detectors were placed on the ground. Three soil moisture sensors (5TM) were buried at 0.10 m below the ground surface.

Key Findings

- The surface CH_4 concentrations demonstrate that the low-cost, near real-time CH_4 detector network, can capture the spatial extent of the surface CH_4 plume with the constant controlled gas leak rate. Additionally, variations in measured surface CH_4 concentrations at each location

exhibit a diurnal pattern, which is influenced by the air temperature and the wind speed during the day and night. An increase in surface temperature promotes turbulence near the surface, facilitating the dispersion of CH_4 from the surface to the atmosphere. On the other hand, higher wind speeds increase atmospheric resistance, impeding the migration of gas from the surface to the atmosphere.

- The experimental results reveal a clear correlation between the increase in gas leak rates and the corresponding rise in surface and belowground near-surface CH_4 concentrations. Furthermore, the plume areas of surface and belowground near-surface CH_4 expands as the leak rates elevated. These findings indicate the effectiveness of the low-cost, near-real-time CH_4 detector network in capturing the evolution and variations of surface and belowground near-surface CH_4 concentrations in scenarios involving different underground natural gas (NG) leak rates. Therefore, the CH_4 detector network proves instrumental in monitoring and tracking the dynamic behavior of CH_4 emissions, enabling a comprehensive understanding and assessment of the impact of varying environmental conditions on the behavior of belowground NG leakage.
- The observed differences in concentrations and plume areas between surface and belowground near-surface CH_4 concentration not only present the influence of atmospheric variability on the evolution of surface CH_4 migration but also indicate the importance of belowground near-surface CH_4 measurements in the quantification of belowground NG leak rates.

Deliverable 3: Field Experiments with the Industry Partner

Objective

- Field experiments are being conducted in collaboration with our industry partner to validate the effectiveness of the low-cost, near-real-time CH_4 network and simulation algorithm. The field data collected is being compared with the simulation results, aiming to test and refine both the network and algorithm. The objective is also to ensure their applicability to various pipeline leakage in both rural and urban scenarios. This validation process enhances the reliability and accuracy of the CH_4 detector network and simulation algorithm, advancing their utility in real-world situations, and providing valuable insights for pipeline safety management in diverse settings.

Experimental Site

The field testing was conducted in collaboration with our industry partner, specifically collecting data from natural gas distribution pipeline leaks (Table 2). Figure 17 illustrates the framework of the field testing, which involved utilizing the low-cost, near-real-time CH_4 detector network. The collected data served the purpose of evaluating the capabilities of both the low-cost, near real-time CH_4 detector network and an inversion algorithm designed for estimating non-steady belowground NG leak rates through the inverse gas migration model. The primary objective was to assess the applicability of the low-cost, near-real-time CH_4 detector network and the inversion algorithm under diverse field conditions. Furthermore, the findings from this field testing were utilized to refine and enhance the framework of the detector network and the inversion algorithm. It is important to note that due to the absence of subsurface leak investigation and repair excavation before the field testing, the precise location of the leaks was not identified. Consequently, the leak location was determined based on the highest surface CH_4 concentration recorded by the handheld detector (DP-IR+) at each field site.

The industry partner and the project team hosted field testing, providing a list of leak sites and access to the selected locations. The selection criteria for leak sites included surface condition (unsurfaced/dirt), migration extent (minimum 4' × 4'), and initial methane readings (≥ 10,000 ppm) reported by the industry partner. Project team conducted comprehensive measurements at seven selected sites (Table 2). Upon arrival at each test site, the study team employed the DP-IR+ (Heath Consultants Inc.) to identify the highest surface concentration reading. Subsequently, CH_4 detectors were strategically deployed in a concentric circle around the estimated leak location, with distances between detectors ranging from 0.5 m to 1 m. Concentration readings were recorded by the CH_4 detectors at 5-second intervals. A portable weather sensor (ATMOS41, METER Group Inc.) and soil moisture and temperature sensors (5TM and EC-5, METER Group Inc.) were installed to record atmospheric variation and soil moisture/temperature at 30-second intervals. Specifically, three soil moisture and soil temperature sensors were placed at a depth of 5 to 10 cm below the ground surface (Figure 18).

All data were collected over a period of 2 hours and subsequently processed using the developed inversion algorithm in this study to determine the non-steady belowground NG leakage rate. To validate the accuracy of the proposed inversion algorithm, the leakage rates were independently measured using a high-flow sampler (SEMTECH HI-FLOW 2, Sensors Inc.). The experimental duration at each test location encompassed approximately 4 hours.

Table 2. Overview of field testing at the testing locations with the industry partner.

Site Number	Duration	Surface Condition
#1	3.5 hours	Soil, grass, and partial sidewalk
#2	3.5 hours	Soil, grass, and partial sidewalk
#3	2.5 hours	Soil, grass, and partial sidewalk
#4	2.5 hours	Soil, grass, and partial underground construction
#5	2 hours	Soil, grass, tree, and partial sidewalk
#6	2 hours	Soil, grass, tree, and partial sidewalk
#7	3 hours	Soil, grass, and partial road surface

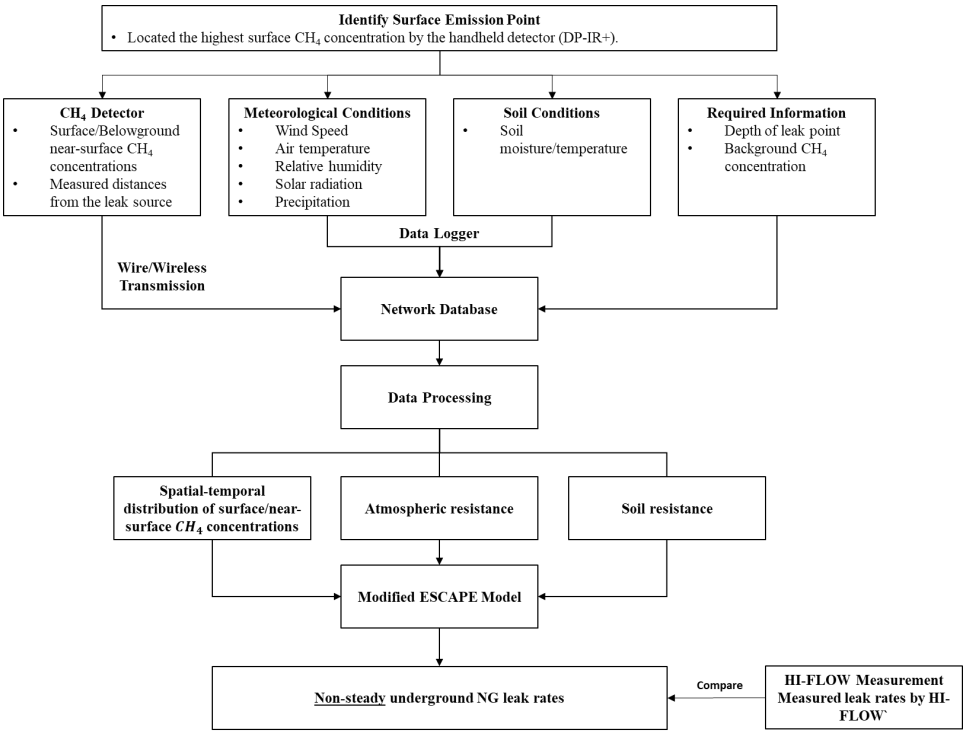

Figure 17. The framework of applying the low-cost near real-time CH_4 detector network to determine the underground non-steady NG leak rates in the field testing.

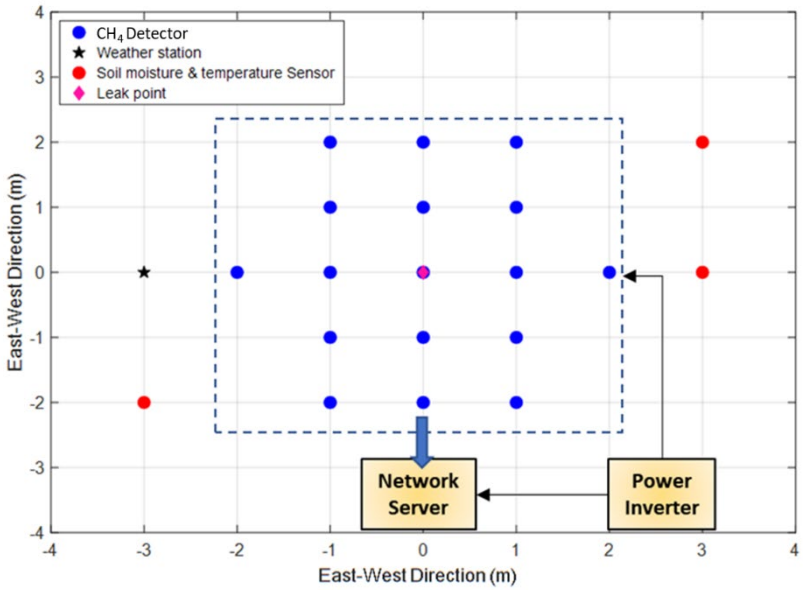

Figure 18. The deployment of natural gas detectors (blue points), the weather station (black star), and the soil moisture/temperature sensors (red points) around the leak location (pink diamond). The leak location is approximated based on the highest surface reading by DP-IR+. The distance between each detector can be adjusted based on the site conditions. All NG detectors are connected to the network server and transmit data to the server. The power inverter provides power to the network server and natural gas detectors.

Measured NG leak rates by the Low-cost, Near Real-time CH_4 Detector Network

Figure 19 presents the distribution of surface and belowground near-surface CH_4 concentrations measured at each testing location. Notably, the range of surface CH_4 concentrations presents a smaller variation compared to the belowground near-surface CH_4 concentrations. This discrepancy can be attributed to environmental conditions, atmospheric stability, and the presence of a surface impermeable cover. The impermeable surface cover (e.g., road surface and sidewalk) induces the lateral gas migration along the bottom of surface cover and then leads to the accumulation of gas at the bottom of surface cover and the high belowground near-surface CH_4 concentrations at the edges of the road surfaces and sidewalks. Moreover, detectors placed near tree roots and cracks on the road surface monitored high CH_4 concentrations in the testing area. This result indicates that tree roots and surface cracks can create preferential flow paths below the ground, inducing the quick migration of belowground gas leaks to the surface. Furthermore, the highest concentrations initially measured by the industry partner were greater than 10,000 ppm (1%), but when we were at the leak locations, the methane concentrations were much lower ($\leq$ 1,000 ppm). This difference indicates that the leak rates observed in the field could vary over time because the leaks could be intermittent leaks.

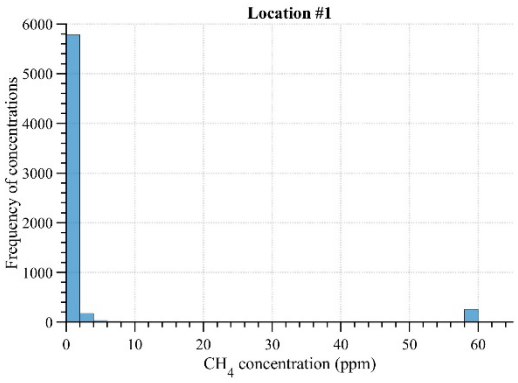
Location #1
Frequency of concentrations
CH4 concentration (ppm)

(a)

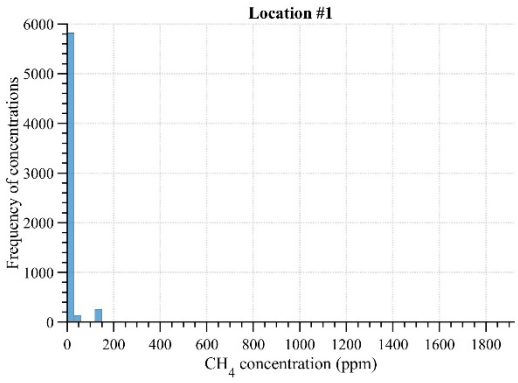
Location #1
Frequency of concentrations
CH4 concentration (ppm)

(b)

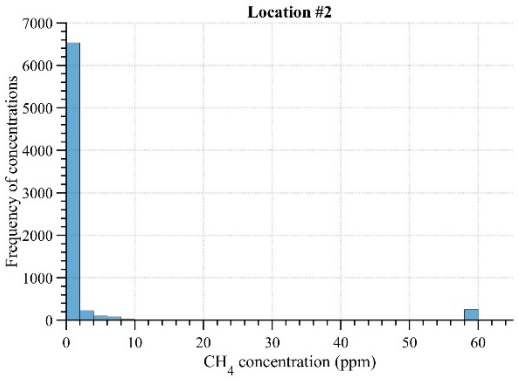
Location #2
Frequency of concentrations
CH4 concentration (ppm)

(c)

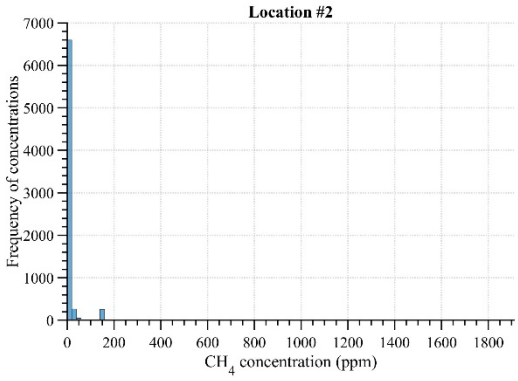
Location #2
Frequency of concentrations
CH4 concentration (ppm)

(d)

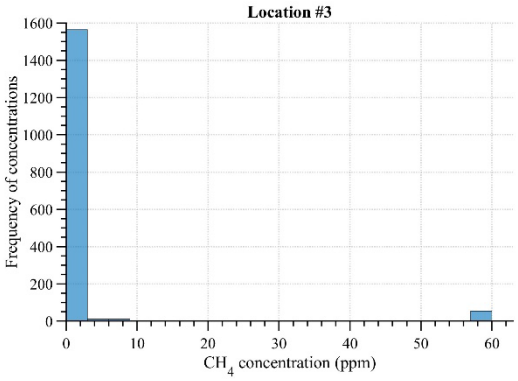
Location #3
Frequency of concentrations
CH4 concentration (ppm)

(e)

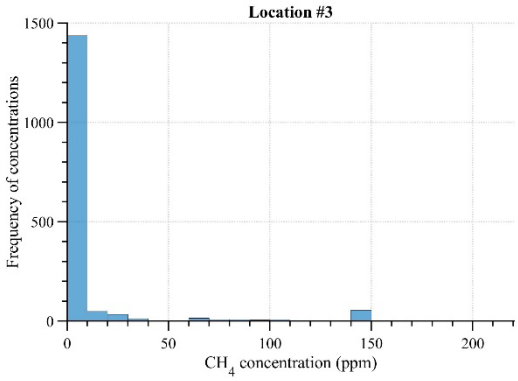
Location #3
Frequency of concentrations
CH4 concentration (ppm)

(f)

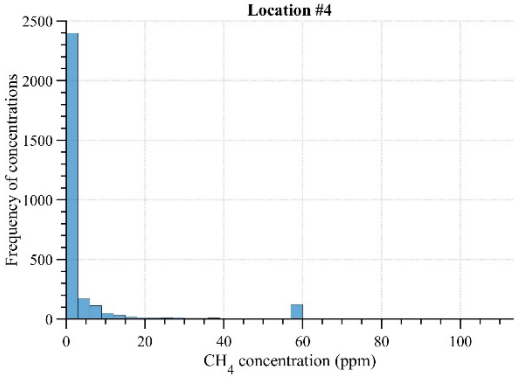
Location #4
Frequency of concentrations
CH4 concentration (ppm)

(g)

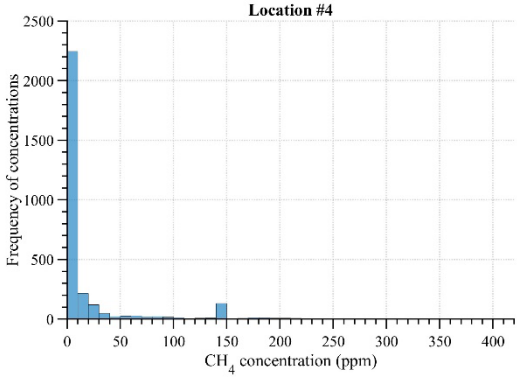
Location #4
Frequency of concentrations
CH4 concentration (ppm)

(h)

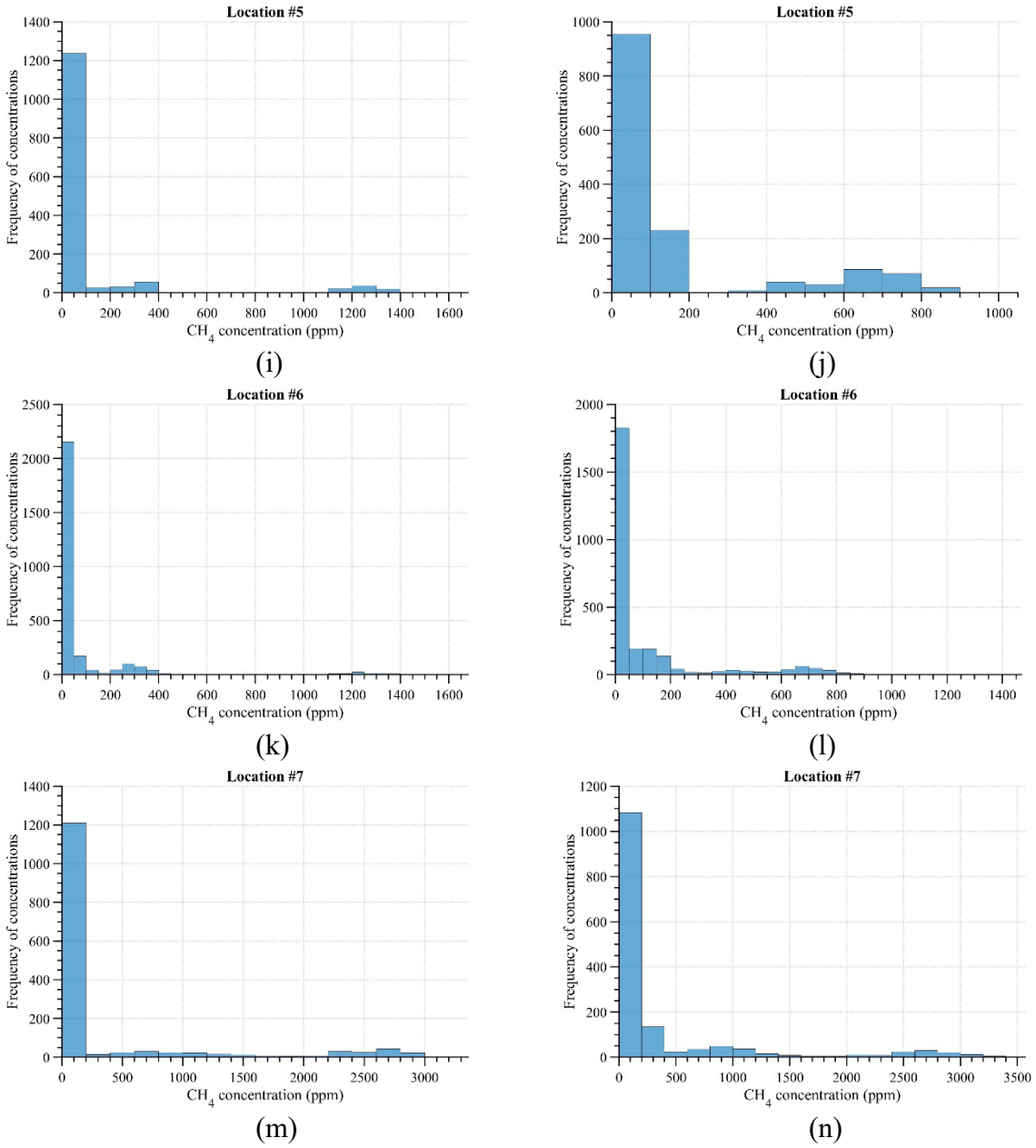

Figure 19. Distribution of surface (a, c, e, g, i, k, and m) and BNS (b, d, f, h, j, l, and n) CH_4 concentrations measured by the low-cost near real-time CH_4 detector network at Locations #1 to #7. Locations #1 to #3 are in soil, grass, and partial sidewalk area. Location #4 includes soil, grass, and partial underground construction. Locations #5 and #6 are in the soil, grass, and partial sidewalk. Location #7 is the soil, grass, and partial road surface area.

Measured NG Leak Rates by the Methane Analyzer

The leakage rates estimated at each location using the methane analyzer (SEMTECH HI-FLOW 2, Sensors Inc.) are summarized in Table 3 and Figure 20. Based on the determination of the gas leak level from the industry partner, the estimated leak rate smaller than 9.3 (g CH_4 hr^{-1}) is a very low leak rate, between 9.3 to 15 (g CH_4 hr^{-1}) is a low leak rate, and from 15 to 90 (g CH_4 hr^{-1}) is a medium leak rate. Therefore, among the seven measured locations, four of them (Location #2, #3, #4, and #5)

exhibited very low leak rates, two measured locations (Location #1 and #6) were low leak rates, and one measured location (Location #7) was medium leak rates.

Table 3. Average leak rates (g CH_4 hr^{-1}) with one standard deviation measured by the methane analyzer (SEMTECH HI-FLOW 2) at each location. Locations #1 to #3 are in soil, grass, and partial sidewalk area. Location #4 includes soil, grass, and partial underground construction. Locations #5 and #6 are in the soil, grass, and partial sidewalk. Location #7 is the soil, grass, and partial road surface area.

Location #	1	2	3	4	5	6	7
Surface 1 leak rate (g CH_4 hr^{-1})	5.02 ± 0.93	0.74 ± 0.19	2.98 ± 0.74	0.19 ± 0.00	5.58 ± 1.30	11.72 ± 2.05	34.79 ± 4.46
Surface 2 leak rate (g CH_4 hr^{-1})	10.42 ± 0.93	0.37 ± 0.19	3.53 ± 0.74	1.12 ± 0.74	3.53 ± 0.74	4.10 ± 0.93	27.53 ± 2.79
Surface 3 leak rate (g CH_4 hr^{-1})	-	-	-	-	-	2.60 ± 0.37	25.30 ± 5.02
Total leak rate (g CH_4 hr^{-1})	15.44	1.11	6.51	1.31	8.93	18.42	87.62
Leak Level	Low	Very Low	Very Low	Very Low	Very Low	Low	Medium

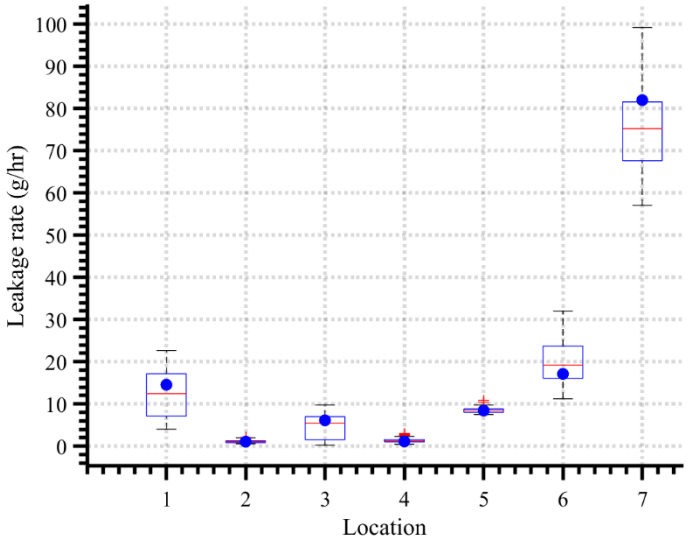

Figure 20. The leakage rates (g CH_4 hr^{-1}) were measured by the methane analyzer (SEMTECH HI-FLOW 2, Sensors Inc.) from Locations #1 to #7. Locations #1 to #3 are in soil, grass, and partial sidewalk area. Location #4 includes soil, grass, and partial underground construction. Locations #5 and #6 are in the soil, grass, and partial sidewalk. Location #7 is the soil, grass, and partial road surface area. The blue point indicates the estimated total leak rate. The red line presents the median total leak rate in measurements.

Key Findings

- The CH_4 concentration varied significantly between discovery and measurements. At initial discovery, the surface CH_4 concentration was greater than 10,000 ppmv, but while conducting measurements, the surface CH_4 concentration was less than 1,000 ppmv. This difference indicates that the leak rates could be changed and vary significantly over time.
- The impermeable surface covers, such as road surfaces and sidewalks, were found to induce lateral gas migration in the belowground near-surface, leading to the accumulation of gas and high belowground near-surface CH_4 concentrations at the edges of road surfaces and sidewalks.
- The presence of cracks in road surfaces and tree roots was identified as a significant factor contributing to preferential flow paths for belowground near-surface CH_4 migration. This observation is supported by the detection of high CH_4 concentrations in the vicinity of these crack and tree root areas. These findings suggest that the cracks in road surfaces and tree roots create pathways that facilitate the migration of CH_4 from below the ground to the near-surface environment.
- The measurements conducted using both the low-cost, near-real-time CH_4 detector and the HI-FLOW 2 highlight the importance of considering environmental factors, surface conditions, and potential migration pathways when evaluating underground gas leakage. These measurements emphasize the complex relationship between environmental conditions, surface characteristics, and the behavior of CH_4 migration. Factors such as atmospheric stability, weather conditions, impermeable covers, and cracks in surfaces play a significant role in influencing the accumulation and migration of CH_4.

Deliverable 4:
Quantifying the Non-steady State Belowground NG Leak Rate – Modified ESCAPE Model

Objective

- Develop a model to effectively and efficiently quantify the belowground natural gas (NG) leak rates.

Modified ESCAPE Model

The original Estimating the Surface Concentration Above Pipeline Emissions (ESCAPE) Model (Riddick et al., 2021) was modified to incorporate the belowground soil properties and gas migration to quantify the non-steady belowground NG leak rates. The modified ESCAPE model does not consider the influence of impermeable surface cover (e.g., asphalt) on the gas migration in the subsurface. In the modified ESCAPE model, the gas flow (CH_4 and air) in the unsaturated soil is assumed to be transported under isothermal conditions. The dissolution of CH_4 in soil water is ignored due to its low solubility in water (0.022 mg/mL) and low water saturation in the below-ground near-surface. The modified ESCAPE model does not incorporate the scenario of heterogeneous surface covers, particularly the impermeable surface cover (e.g., concrete or asphalt) that may significantly impede the diffusion of gas, resulting in extensive migration over long distances before reaching an active atmospheric interface.

In the modified ESCAPE model, the non-study belowground NG leak rate is described by a summation of the steady belowground NG leak rate ($\overline{Q_L}$) from the original ESCAPE model and the non-steady NG leak rate dominated by surface and belowground near-surface environmental conditions (Eq. 1).

$$Q_L(t) = \overline{Q_L} + Q_{LT}(R_s, R_a, C_s, C_{ns}, x, t) \tag{1}$$

where Q_L (g/h) is the non-steady NG leak rate from the underground pipeline, $\overline{Q_L}$ (g/h) is the steady belowground NG leak rate estimated by the original ESCAPE model [Riddick et al., 2021], and Q_{LT} (g/h) is the NG leak rate under non-steady conditions. The steady belowground NG leak rate by the original ESCAPE model can be estimated by the difference between surface and background CH_4 concentrations and the atmospheric resistance on an equivalent area of CH_4 flux (Eq. 2).

$$\overline{Q_L} = A_e(x)\frac{\sum_{i=1}^{\infty}\frac{1}{\sqrt{x_i^2+d^2}}}{\frac{1}{\sqrt{x_i^2+d^2}}}\frac{C_s(x,t)-C_a}{R_{at}(t)} \tag{2}$$

where the subscript i represents the location of surface measurements, d (m) is the depth of the leak point (d, m), and A_e (m^2) is the equivalent area of CH_4 flux. The equivalent area of CH_4 flux (A_e) did not change over time because the distance (x) is fixed based on the location of measurement. Thus, the equivalent area of CH_4 flux (A_e) can be described based on the location of measurements:

$$A_e(x) = \pi \left[\left(\frac{x_{i+1} - x_i}{2} \right)^2 - \left(\frac{x_i - x_{i-1}}{2} \right)^2 \right] \quad (3)$$

The non-steady change in NG leak rate (Q_{LT}) reflects the gas migration from the subsurface to the surface. The soil resistance (R_s), the atmospheric resistance (R_a), and spatial-temporal surface/near-surface methane concentrations (C_s and C_{ns}) are required to calculate surface gas emission rates (Q_s) over time.

Soil resistance (R_s)

Previous studies indicated that soil resistance is strongly related to soil moisture and presented multiple soil surface resistance models [Shu Fen,1982; Camillo and Gurney, 1986; van de Griend and Owe,1994]. Bittelli et al. (2008) indicated that the model proposed by van de Griend and Owe (1994) showed the best estimation of evaporation. Therefore, we selected the model of van de Griend and Owe (1994) to describe the soil resistance of the topsoil at the site (Eq. 4) [van de Griend and Owe, 1994; Li, 2020].

$$R_s(t) = R_{sl} e^{0.3563(\theta_{min} - \theta_{top})} \quad (4)$$

where R_{sl} (s/m) the resistance to molecular diffusion across the water surface, which was given 10 (s/m), θ_{min} (m^3/m^3) is empirical minimum soil moisture which the soil can deliver vapor at a potential rate, which was given 0.18 in this study, and θ_{top} is the soil moisture content in the topsoil.

Aerodynamic resistance (R_a)

The aerodynamic resistance (R_a) can be estimated using several parameters, including the roughness length (z_0), the displacement length (z_d), the Monin-Obukhov length (L), the von Karman constant (k = 0.41), the wind speed at a height of z meters above the ground surface (u_z), and a stability correction function (ψ_m) [Nemitz et al., 2000; Seinfeld and Pandis, 2016]. In this study, the roughness length (z_0) was determined to be 0.05 m, while the displacement length (z_d) was 0.01 m based on the environmental conditions of the test site. The stability correction function was defined using Eq. 6 for stable conditions and Eq. 7 for unstable conditions. The aerodynamic resistance (R_a) increases during stable conditions, which occur under low wind and low solar radiation conditions. Conversely, high wind and high solar radiation induce unstable conditions, leading to a decrease in R_a.

$$R_a = \frac{\left[\ln\left(\frac{z - z_d}{z_0} \right) - \psi_m \left(\frac{z - z_d}{L} \right) \right]^2}{k^2 u_z} \quad (5)$$

Stable Condition ($L > 0$):

$$\psi_m \left(\frac{z - z_d}{L} \right) = -\frac{5z}{L} \quad (6)$$

Unstable Condition ($L < 0$):

$$\psi_m \left(\frac{z - z_d}{L} \right) = 2 \ln\left(\frac{1 + X}{2} \right) + \ln\left(\frac{1 + X^2}{2} \right) - 2 \tan^{-1}(X), \quad (7)$$

$$where\ X = \left(1 - 16 \frac{z}{L} \right)^{\frac{1}{4}}$$

where z is the height of measurement of weather conditions (m), z_0 is the roughness length (m), z_d the displacement length (m), L is the Monin-Obukhov length (m), k is the von Karman constant (k = 0.41), u_z is the wind speed at the height z m (m/s), and ψ_m is a stability correction function.

Boundary layer resistance (R_b)

The boundary layer resistance (R_b) can be calculated using Eq. 8. The Schmidt number for mass transfer (Sc) is determined by the ratio of the kinematic viscosity to the molecular diffusivity of water vapor in the air. For this study, Sc was approximately 0.7. The kinematic viscosity of air (v) is temperature dependent. The upper height of the logarithmic wind profile above the ground surface (z_l) was assumed to be the height of the local weather station at the test site [Nemitz et al., 2000; Schuepp, 1977].

$$R_b = \frac{Sc - \ln\left(\frac{v}{ku_*}/z_l\right)}{ku_*} \tag{8}$$

where R_b is the boundary layer resistance (s/m), Sc is the Schmidt number for mass transfer (-), v is the kinematic viscosity of air (m^2/s), z_l is the height of the measurement of weather conditions (m), and u_* is the wind friction velocity (m).

The atmospheric resistance (R_{at}, s/m) can be described as the summation of the aerodynamic resistance (R_a, s/m) and the boundary layer resistance (R_b, s/m) (Eq. 9).

$$R_{at} = R_a + R_b \tag{9}$$

Modeled Non-steady NG Leak Rates in Controlled NG Release Experiment at METEC

With the data collected from the low-cost near real-time CH_4 detector network, the non-steady NG leak rates were calculated by the modified ESCAPE model (Figure 21). When the average of true rates and modeled NG rates were compared, the differences ranged from 3.80% to 11.87% with an average of 7.99% (Table 4). The modeled NG leak rate were 32.67 ± 4.56 (g CH_4 h^{-1}), 98.21 ± 24.99 (g CH_4 h^{-1}), 114.13 ± 23.67 (g CH_4 h^{-1}), and 197.70 ± 116.81 (g CH_4 h^{-1}) in levels 1, 2, 3, and 4 (Figure 22). Three increased trends of the modeled non-steady NG leak rates occurred at hours 53, and 85, while a decreased trend appeared from hour 102 to hour 120 in level 3 and retained an averaged NG leak rate of 94.07 (g CH_4 h^{-1}). The overall modeled non-steady NG leak rates from levels 1 to 3 by the modified ESCAPE model were in better agreement (R^2=0.77 and m=0.99). This was also supported by the lower standard deviations and differences observed between the modeled and true NG leak rates at gas leak scenarios from levels 1 to 3, as shown in Table 4. The third increased trend occurred after the third increase in the controlled NG leak rate (hour 124). However, there is a significant increase appearing at hour 150. According to the change in the soil moisture and soil resistance (Figure 23), this dramatical increase may be induced by the sudden increase in the soil moisture inducing the decrease in soil resistance. The decrease in the soil resistance could increase the estimated non-steady NG leak rates in the modified ESCAPE model (Eq. 1). Therefore, the precipitation is an improved factor in the modified ESCAPE model in further research for accurately capturing the changes in belowground NG leak rates.

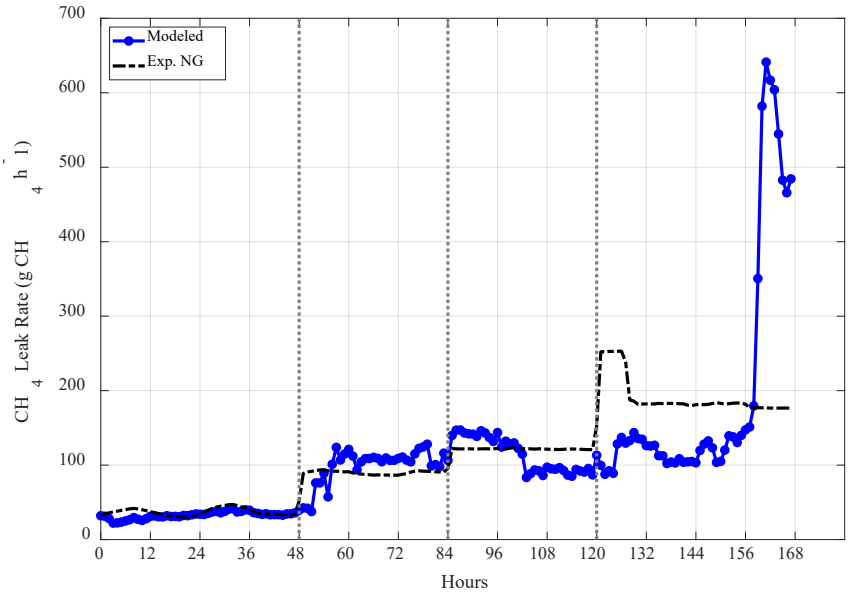

Figure 21. Comparison of true emission rates and modeled NG leak rates by the modified ESCAPE model during the controlled NG release experiment at METEC. The gray dotted lines indicate the time when average controlled NG release rates (g CH_4 hr^{-1}) were increased from 37.08 (g CH_4 hr^{-1}) to 88.76 (g CH_4 hr^{-1}) at hour 48, from 88.76 (g CH_4 hr^{-1}) to 120.96 (g CH_4 hr^{-1}) at hour 84, and from 120.96 (g CH_4 h^{-1}) to 190 (g CH_4 h^{-1}) at hour 120.

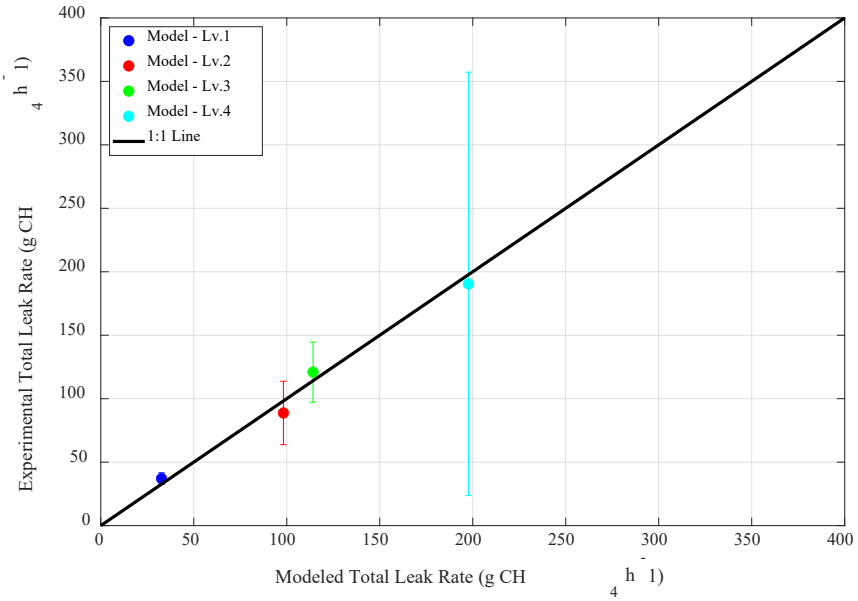

Figure 22. A comparison between the experimental total leak rate gas rate and the modeled total leak rate estimated by the inverse gas migration model (circle) in each NG leak scenario. The black line presents the 1:1 line.

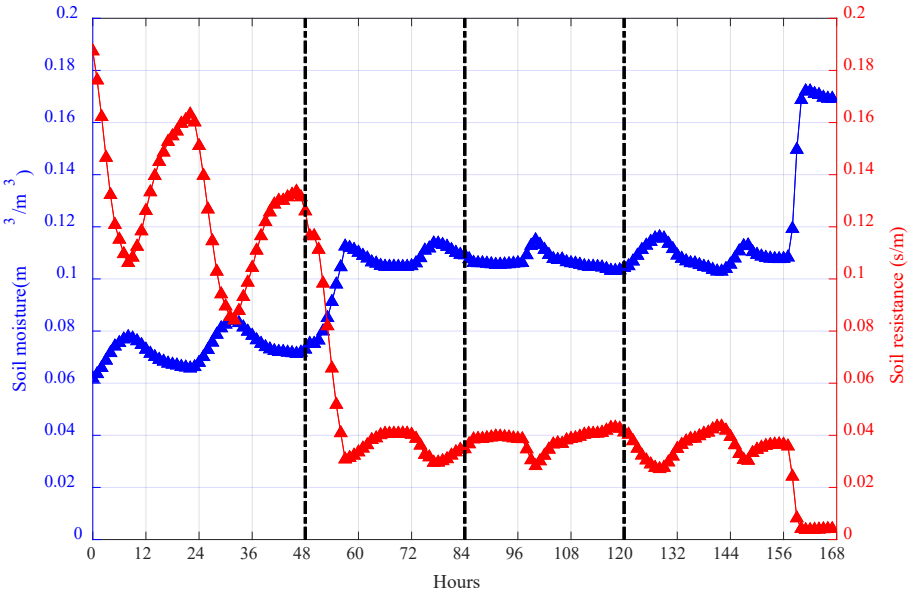

Figure 23. Comparison of soil moisture and soil resistance during the controlled NG release experiment at METEC. The black dotted lines indicate the time when controlled NG release rates (g CH_4 hr^{-1}) were increased from 37.08 (g CH_4 hr^{-1}) to 88.76 (g CH_4 hr^{-1}) at hour 48, from 88.76 (g CH_4 hr^{-1}) to 120.96 (g CH_4 hr^{-1}) at hour 84, and from 120.96 (g CH_4 h^{-1}) to 190 (g CH_4 h^{-1}) at hour 120.

Table 4. A summary of the estimated non-steady NG leak rate from both the ESCAPE and the modified ESCAPE model in each NG leak rate scenario. The "Std." column shows the standard deviation for each model, while the "difference" column indicates the percentage difference between the experimental and modeled total leak rate.

NG Release Rate Level		Experimental Averaged Leak Rate (g CH_4 hr^{-1})	Modeled Averaged Leak Rate (g CH_4 hr^{-1})	Std. (g CH_4 hr^{-1})	Difference (%)
Modified ESCAPE	Lv. 1	37.07	32.67	4.56	11.87
	Lv. 2	88.76	98.21	24.99	10.65
	Lv. 3	120.96	114.05	23.55	5.71
	Lv. 4	190.47	197.70	166.81	3.80

Modeled Non-steady NG Leak Rates in Field Testing with the Industry Partner

Among the seven study sites, the four sites (Location # 2, 3, 4, and 5) had very low leak rates (< 9 g CH_4 hr^{-1}), two sites (Location #1 and 6) presented low leak rates (leak rates between 9 g CH_4 hr-1 to 37 g CH_4 hr^{-1}), and one site (Location #7) showed medium leak rates (leak rates between 39 g CH_4 hr-1 to 186 g CH_4 hr^{-1}) based on the measurements from the high flow sampler (Figure 20).

When the measurements of leak rates of the seven sites by the methane analyzer (SEMTECH HI-FLOW 2, Sensors Inc.) were compared to the estimations of non-steady belowground NG leak rate

by the modified model, the difference in gas leak rate was 6.56% at Location #1, 14.33% at Location #2, 79.69% at Location #3, 469.57% at Location #4, 15.65% at Location #5, 7.46% at Location #6, and 0.09% at Location #7 (Table 5). Furthermore, when the gas leak rates were higher than 9.28 (g CH_4 hr^{-1}) (Location #1, 6, and 7), the modified ESCAPE model demonstrates good field application with reasonable accuracy, and the differences were smaller than 10%. However, when the gas leak rates were smaller than 9.28 (g CH_4 hr^{-1}) (Locations #2, #3, #4, and #5), the modified ESCAPE model presented a higher difference of over 10%. At Location #4, the difference in gas leak rates reached 469.57%. We speculated that there were some unidentified structures below the iron sheet area that impacted the simulation of the inverse model and the measurements.

Table 5. Measurements of gas leakage rates (g CH_4 hr^{-1}) by the HI-FLOW and the modified ESCAPE model at each test site.

Location #	Total NG leak rates by HI-FLOW (g CH_4 hr^{-1})	Total NG leak rates by the modified ESCAPE model (g CH_4 hr^{-1})	Difference of total gas leak rates (%)	Category of gas leakage
1	15.60	16.62	6.56	Low
2	1.11	1.27	14.33	Very Low
3	6.50	1.32	79.69	Very Low
4	1.30	7.40	469.57	Very Low
5	8.91	7.52	15.65	Very Low
6	18.19	16.84	7.46	Low
7	87.26	87.18	0.09	Medium

Key Findings

- The modified ESCAPE model captured and quantified the non-steady belowground natural gas (NG) leak rates with reasonable accuracy (3.80% to 11.87%). This result emphasizes the importance of considering belowground gas migration and soil characteristics when quantifying belowground NG leak rates. However, further improvements are needed to address the influence of rapid increases in soil moisture resulting from precipitation on the estimation of the modified ESCAPE model. Enhancing the ability of the modified ESCAPE model to account for such variations will advance its application in quantifying non-steady belowground NG leak rates.
- The field application of the modified ESCAPE model was successfully assessed for the leak rates between 15 g CH_4 hr^{-1} and 90 g CH_4 hr^{-1} in collaboration with an industry partner. The very low leak rates (< 9 g CH_4 hr^{-1}) may not be able to be determined by the modified ESCAPE model.
- Placing the low-cost near-real-time CH_4 detector around the location of the highest surface CH_4 concentration was an effective way to deploy and determine the leak rates of the pipeline when it was tested in the field.

Deliverable 5: Recommendations to Incorporate Findings into Practice

Objective

- As presented in the above deliverables, this project developed a low-cost, near real-time CH_4 detector network to link measurements of surface/belowground near-surface CH_4 concentrations, weather conditions, and belowground soil characteristics to a modified gas migration model (the modified ESCAPE model) to quantify the non-steady belowground NG leak rates. This section addresses opportunities to incorporate the use of a low-cost, near real-time CH_4 detector network and the modified ESCAPE model into operator practice for leak rate estimates and also offers recommendations for further research, based on the initial findings presented in this project.

Scenario Analysis in the Modified ESCAPE Model

The scenario analysis, which is a process of generating and analyzing different hypothetical scenarios based on varying input parameters in the model, was conducted to study the recommended practice of the low-cost near real-time CH_4 detector. In the modified ESCAPE model, the maximum CH_4 concentration within multiple detectors at a measured distance presented the equivalent CH_4 at this measured distance. Therefore, we selected different combinations of measured distance to study the influences of numbers of measured distance on the estimation of non-steady NG leak rate in the modified ESCAPE model. The normalized root mean squared error (*NRMSE*) (Eq. 10) is used to evaluate the results of the scenario analysis.

$$NRMSE = \frac{RMSE}{mean(y)} \tag{10}$$

where y indicates the measured belowground NG leak rates.

Scenario – Number of Measured Locations

There are 8 different measurement locations in the controlled gas release experiment (Figure 13). Figure 24 shows the changes in the *NRMSE* with the increase of numbers of measurement locations from 2 to 8 locations for gas leak rates from levels 1 to 4, respectively. The non-steady NG leak rate modeled by the modified ESCAPE model was found to agree well with the true NG leak rate as the number of measured distances increased (Figure 24). The *NRMSE* decreased from 4.13 to 0.19 with the leak rate at Level 1, from 2.53 to 0.28 with the leak rate at Level 2, from 1.14 to 0.2 with the leak rate at Level 3, and from 2.91 to 0.91 at Level 4. Furthermore, the *NRMSE* with leak rates at Levels 2 and 3 were slightly higher than that at Level 1 as the number of measured distances increased to 3 and 5, respectively. As the controlled NG leak rate increases, the error between simulated and experimental NG leak rates gradually increases due to heterogeneous soil characteristics and atmospheric variability. Therefore, the accumulated error in the model induces slight differences in NRMSE. Moreover, the NRMSE in Level 4 is much higher than that at other levels of gas leaks. The large difference here is caused by the increase of soil moisture due to precipitation in hour 168 (Figure 23). The significant increase in soil moisture decreased the soil resistance and then enhanced the estimated gas leak in the model. Therefore, although the increase in the number of measured locations could advance the estimated result in the modified ESCAPE model, the precipitation or the change in the soil moisture is a required improvement in further research in the modified ESCAPE model.

In the controlled gas release experiment, the modified ESCAPE model's ability to estimate non-steady belowground NG leak rates was examined at different measured distances. Figure 24 demonstrates that as the number of measured distances increased, the model's agreement with the true NG leak rate improved. The normalized root mean square error (NRMSE) decreased for gas leak rates at levels 1, 2, and 3, indicating better accuracy with more measured distances. However, for gas leak rates at level 4, the NRMSE increased, primarily due to increased soil moisture caused by precipitation. These results suggest that while increasing the number of measured locations enhances the model's estimation, addressing the impact of precipitation and soil moisture is vital for further improvement.

Overall, the study emphasized the significance of considering soil moisture and its variability in accurately quantifying non-steady belowground NG leak rates using the modified ESCAPE model. The findings highlight the need for future research to address the influence of precipitation and changes in soil moisture, as they can affect the accuracy of the model's estimates.

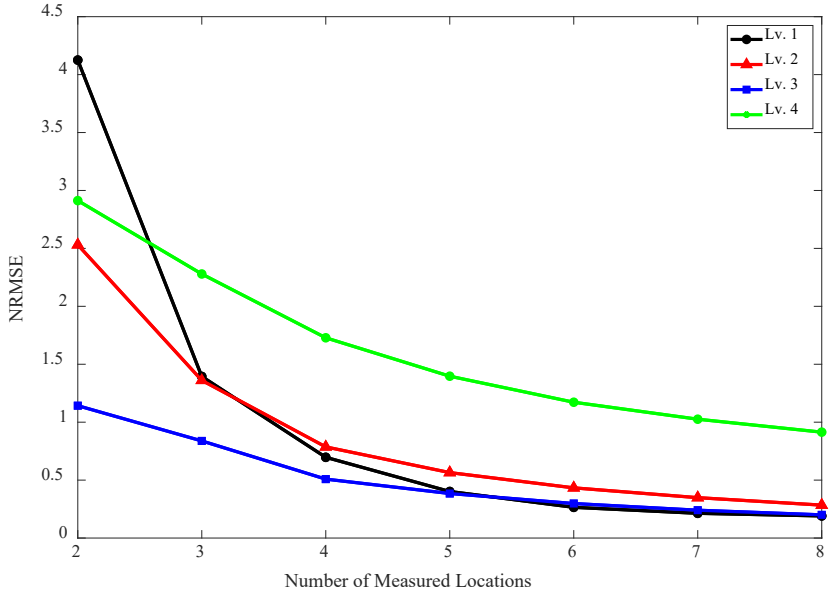

Figure 24. The *NRMSE* with the selected number of measured distances from 2 to 8 in the modified ESCAPE model during the leak rate at Levels 1 to 3.

Scenario – Number of Measured Times

There are 4 different levels in the controlled gas release experiment (Table 4). Figure 25 shows the changes in the *NRMSE* with the increase in the number of measured times in four changes in controlled gas leak rates.

When the controlled gas leak rate remained at Level 1 (37.07 g CH_4 h^{-1}), the *NRMSE* showed a decreasing trend after 7 hours, suggesting that the low-cost, near real-time CH_4 detector network, requires a minimum of 7 hours to obtain proper measurements when the gas leak rate remains constant (Figure 25a). However, when the controlled gas leak rate increased from 37.07 to 88.76 g CH_4 h^{-1}, the NRMSE decreased after only 2 hours, indicating that the proposed detector network can achieve reliable measurements within a shorter time frame after an increase in gas leak rate (Figure 25b). Similarly, when the gas leak rate increased from 88.76 to 120.96 g CH_4 h^{-1}, the *NRMSE* also decreased after 2 hours (Figure 25c). It is worth noting that an increase in *NRMSE* was observed after 18 hours, which may be attributed to precipitation occurring at that time, affecting the surface and BNS CH_4

measurements. In Figure 25d, the NRMSE decreased after 5 hours following an increase in the gas leak rate from 120.96 to 190.47 g CH_4 h^{-1}, but increased after 39 hours, possibly due to precipitation at the 38th hour impacting soil moisture and prolonging the response time for surface and BNS CH_4 measurements. Overall, these findings indicate that the proposed detector network requires 2 to 5 hours to obtain reliable measurements for quantifying non-steady belowground NG leak rates from the pipeline.

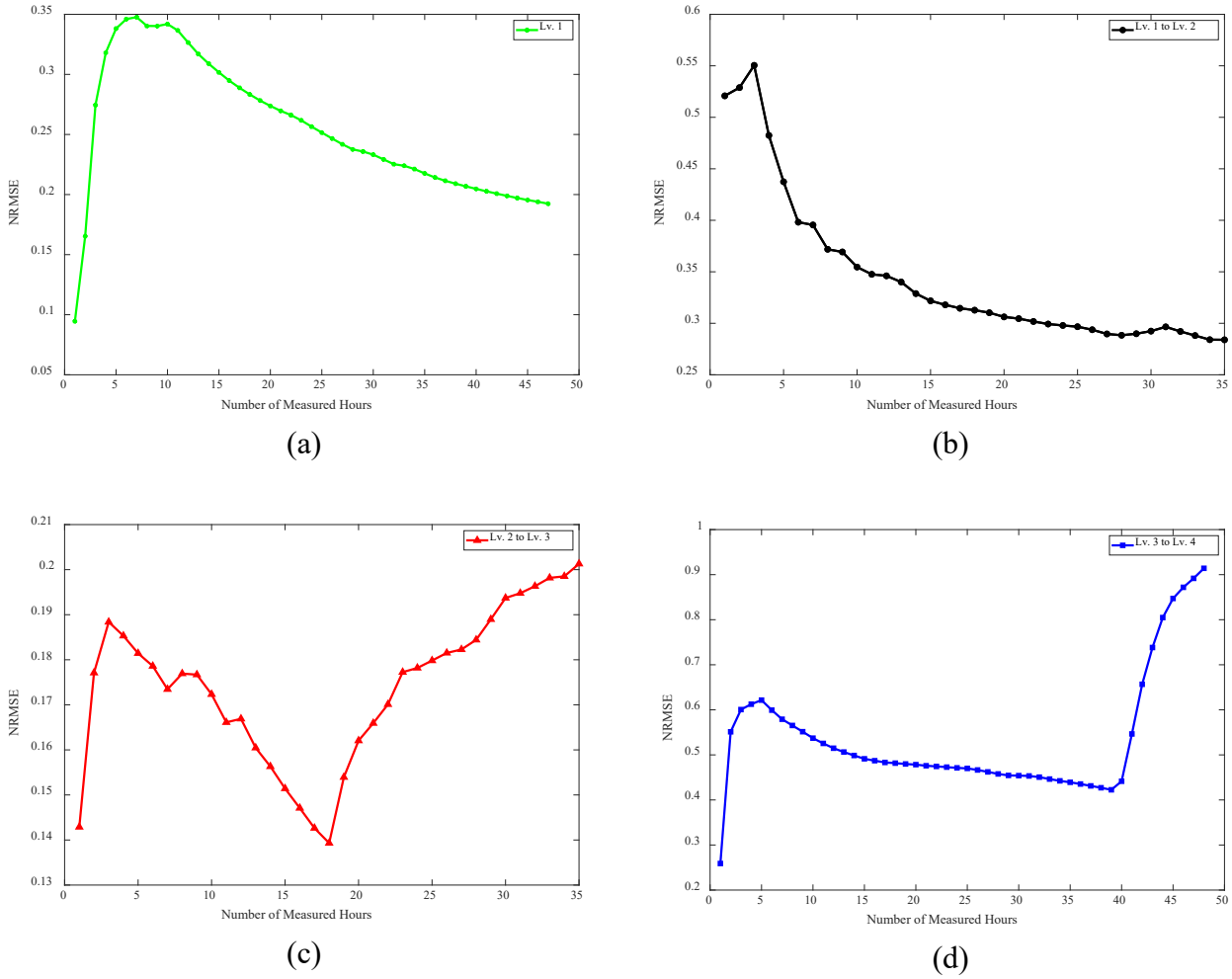

Figure 25. The *NRMSE* with the number of measured times as the controlled gas leak rate (a) in Level 1 (37.07 g CH_4 h^{-1}), (b) increased from Level 1 to Level 2 (from 37.07 to 88.76 g CH_4 h^{-1}), (c) increased from Level 2 to Level 3 (from 88.76 to 120.96 g CH_4 h^{-1}), and (d) increased from Level 3 to Level 4 (from 120.96 to 190.47 g CH_4 h^{-1}) in the modified ESCAPE model.

Scheduled Scenarios of Deployment of CH_4 Detectors in the Detector Network

The measurements of surface and belowground near-surface CH_4 concentrations and the estimation of non-steady belowground NG leak rates indicate that the low-cost near real-time CH_4 detector network and the modified ESCAPE model could capture the evolution of surface and belowground near-surface CH_4 migration and quantify the non-steady belowground NG leak rates under varied NG leak rate and without surface covers scenarios. The project team had meetings with the industry partner to discuss the potential scenarios of the deployment of CH_4 detectors in the detector

network. We suggest the four scenarios with the minimum number of detectors in using the low-cost near real-time CH_4 detector network to appropriately detect and quantify belowground NG leak rates under the complicated surface and subsurface scenarios. The four scenarios in detecting and quantifying the belowground NG leak rate are categorized based on conditions of surface covers and belowground obstruction (e.g., the basement).

1. Permeable Cover (Soil & Grass) without any underground obstructions

The scenario with permeable cover (e.g., soil and grass area) and without the belowground obstruction is used in the previous controlled gas release experiments at METEC. Based on the scenario analysis of the number of measured locations (Figure 24), we suggest using three CH_4 detectors at least to monitor surface and subsurface CH_4 concentrations and to provide reliable data to the modified ESCAPE model to estimate the non-steady belowground NG leak rate.

The measured locations of CH_4 detectors should be at

- The potential leak point is determined with the highest surface CH_4 concentration by the handheld sensor (e.g., DPIR+). The determined leak point is the center of the low-cost, near real-time CH_4 detector network in the detection.
- The boundary of the potential CH_4 plume which is determined with the lowest surface CH_4 concentration (e.g., close to 0 ppm) by the handheld sensor (e.g., DPIR+)
- The proposed measure distances between the determined leak point and the boundary of the plume.

2. Impermeable Cover (Pavement) without underground obstruction

The scenario with impermeable cover (e.g., pavement) and without the belowground obstruction is used to understand the influence of only impermeable cover on the gas migration from the leak source to the surface. Similarly, we need to deploy detectors at the determined leak point and boundary of plum and the proposed measured distance. In addition, we plan to deploy one or two additional detectors at the boundary of the pavement and the cracks on the pavement (i.e., 4 or 5 CH_4 detectors at least).

The measured locations of CH_4 detectors should be at

- The potential leak point is determined with the highest surface CH_4 concentration by the handheld sensor (e.g., DPIR+). The determined leak point is the center of the low-cost, near real-time CH_4 detector network in the detection.
- The boundary of the potential CH_4 plume which is determined with the lowest surface CH_4 concentration (e.g., close to 0 ppm) by the handheld sensor (e.g., DPIR+)
- The proposed measure distances between the determined leak point and the boundary of the plume.
- The boundary of pavement can be used to help us understand the influence of pavement on the belowground gas migration.
- The cracks on the pavement (if occur) can be utilized to understand if the crack could be the preferential flow path in the belowground gas migration.

3. Permeable Cover (Soil & Grass) with underground obstruction

The scenario with permeable cover (e.g., soil and grass area) and the belowground obstruction is used to understand the influence of only belowground obstruction (e.g., the

basement) on the gas migration from the leak source to the surface. Similarly, we need to deploy detectors at the determined leak point and boundary of plum and the proposed measured distance. In addition, we plan to deploy one additional detector close to (or in) locations of any potential belowground structures.

The measured locations of CH_4 detectors should be at

- The potential leak point is determined with the highest surface CH_4 concentration by the handheld sensor (e.g., DPIR+). The determined leak point is the center of the low-cost, near real-time CH_4 detector network in the detection.
- The boundary of the potential CH_4 plume which is determined with the lowest surface CH_4 concentration (e.g., close to 0 ppm) by the handheld sensor (e.g., DPIR+)
- The proposed measure distances between the determined leak point and the boundary of the plume.
- The locations that are close to (or in) any potential belowground structures to help us understand the influence of belowground structures on the belowground gas migration.

4. Impermeable Cover (Pavement) with underground obstruction

The scenario with impermeable cover (e.g., soil and grass area) and the belowground obstruction (e.g., basement) is used to understand the influence of impermeable surface cover and belowground obstruction (e.g., the basement) on the gas migration from the leak source to surface. Similarly, we need to deploy detectors at the determined leak point and boundary of plum and the proposed measured distance. In addition, we schedule to deploy three additional detectors at least at the boundary of the pavement, the cracks on the pavement, and the location that is close to (or in) locations of any potential belowground structures.

The measured locations of CH_4 detectors should be at

- The potential leak point is determined with the highest surface CH_4 concentration by the handheld sensor (e.g., DPIR+). The determined leak point is the center of the low-cost, near real-time CH_4 detector network in the detection.
- The boundary of the potential CH_4 plume which is determined with the lowest surface CH_4 concentration (e.g., close to 0 ppm) by the handheld sensor (e.g., DPIR+)
- The proposed measure distances between the determined leak point and the boundary of the plume.
- The boundary of pavement can be used to help us understand the influence of pavement on the belowground gas migration.
- The cracks on the pavement (if occur) can be utilized to understand if the crack could be the preferential flow path in the belowground gas migration.
- The locations that are close to (or in) any potential belowground structures to help us understand the influence of belowground structures on the belowground gas migration.

Key Findings

- Three CH_4 detectors are the minimum required number of detectors in the low-cost near real-time CH_4 detector network to detect the evolution of surface and belowground near-surface CH_4 concentrations and quantify the non-steady belowground NG leak rates under the permeable cover without underground obstruction scenario.

- Two to five hours is the minimum required measured time in the low-cost near real-time CH_4 detector network to detect the evolution of surface and belowground near-surface CH_4 concentrations and quantify the non-steady belowground NG leak rates under the permeable cover without underground obstruction scenario.

- Based on the discussion with industry partners, we recommended four scenarios that could be scheduled to validate the capability of the low-cost near real-time CH_4 detector network on detection, localization, and quantification of belowground NG leak rates under different environmental conditions.

Based on the research presented in this report, we recommend the following areas for further research and investigation:

- The initial findings from experiments in this project highlight the importance of considering belowground near-surface measurements of CH_4 concentration and soil characteristics in the detection and quantification of belowground NG leakage. However, it should be noted that in this project, subsurface measurements were limited to a depth of 10 cm below the ground surface, without monitoring the change of soil moisture and temperature with depth. To gain a comprehensive understanding of subsurface gas migration, it is crucial to investigate the spatial and temporal variations of soil moisture and temperature. This aspect represents a key area for future research and holds significance in practical applications related to the detection and quantification of belowground NG leakage.

- The estimation of non-steady belowground NG leak rates using the modified ESCAPE model highlights the influence of soil moisture on the accuracy of the estimates. It is observed that a significant increase in soil moisture leads to a decrease in soil resistance and subsequently results in an overestimation of the leak rate. However, a crucial aspect that remains unclear is determining the appropriate range of soil moisture for accurate estimation using the modified ESCAPE model. One of the main uncertainties in the estimation process is the absence of a model that adequately describes gas migration in highly saturated soil conditions. Therefore, to effectively apply the modified ESCAPE model in complex environmental conditions, it is essential to further investigate the impact of precipitation and changes in soil moisture on subsurface gas migration. This area represents a key focus for future research.

- The scenario analysis conducted with varying numbers of measured locations and times reveals that short-term measurements taken on the surface and subsurface (e.g., 2 to 5 hours) have the potential to provide accurate estimations of underground leak rates. However, it is important to note that these findings were obtained in soil and grass areas. To gain a comprehensive understanding of the minimum requirements for measured locations and times, further research should conduct controlled gas release experiments with impermeable surface covers such as pavement and belowground obstructions such as basements. By expanding the scope of the experiments to include these different scenarios, a more advanced assessment can be made to determine the optimal number of measured locations and times for accurate estimation of underground leak rates.

- Research presented here suggests additional and warranted research in estimating belowground NG leak rates.

    - The modified ESCAPE model, a simple analytic tool, can estimate belowground NG leak rates using measurements that are commonly conducted during a leak survey and require minimal soil characteristics. This approach can be integrated into a hand-held device, making it convenient for detection purposes and enhancing its usability and efficiency in detecting and quantifying belowground NG leaks.

    - Measurements of methane (CH_4) concentrations in or around belowground structures or obstructions can provide valuable insights into the impact of NG accumulation in these areas on the performance of low-cost, near real-time CH_4 detector networks in quantifying belowground NG leak rates.

The recommendations above are not all-inclusive as many other factors, such as investigating the effect of trenched bed systems, fractured soils, large surface obstructions, leak orientation, and others were not included in our analysis. They will be addressed in ongoing investigations.

Deliverable 6: Project Outputs

Conference Presentations and Proceedings

1. Cho, Y.*, J. H. Lee , J. Lo , J. Duggan , **K. M. Smits**, and D. Zimmerle. "Natural gas fugitive leak detection and quantification using a continuous methane emission monitoring system and a simplified model" AGU 2022 Fall meeting (Poster)
2. Cho, Y., **K.M. Smits**, S. Riddick, D. Zimmerle, Methane detector network calibration and deployment for monitoring natural gas leaks from buried pipelines, American Geophysical Union Fall Meeting, Dec 2021 (Poster)
3. Cho, Y.*, J. H. Lee , J. Lo , J. Duggan , **K. M. Smits**, and D. Zimmerle. "Natural gas fugitive leak detection and quantification using a continuous methane emission monitoring system and a simplified model" American Geophysical Union (AGU) Fall Meeting, 12 - 16 December 2022, Chicago, Illinois. (Poster)
4. **K. M. Smits**, Cho, Y., J. Duggan, and J. Lo. Improving pipeline safety during gas leakage events using near real-time data networks and decision-making tools" PRCI Pipeline Research Council International REX 2023 conference Submitted (Presentation)
5. Lo, J *, **K.M. Smits**, Y. Cho, J. Duggan, S. Riddick, Utilizing the Near Real-Time Methane Detector Network to Study and Quantify Underground Natural Gas Leakage from the Pipeline, CH4 Connections conference, Oct 20-21, 2022 (Poster)
6. Lo, J *, **K.M. Smits**, Y. Cho, J. Duggan, S. Riddick, Utilizing the Near Real-Time Methane Detector Network to Study and Quantify Underground Natural Gas Leakage from the Pipeline, American Geophysical Union Fall Meeting, Dec 2022 (Poster)
7. Lo, J**, K.M. Smits**, Cho, Y., J. Duggan, C. Horst, L. Aldana, Development and Application of Remote, Near Real-Time Methane Detector Network for Belowground Pipeline Leaks, Energy Institute Publications
8. Lo, J.*, **K.M. Smits**, Cho, Y., J. Duggan, S. Riddick, Utilizing the Near Real-Time Methane Detector Network to Study and Quantify Underground Natural Gas Leakage from the Pipeline, GTI/CSU CH4 Connections conference, Oct 20-21, 2022 (Poster)
9. Lo, J., K.M. Smits, Cho, Y., J. Duggan, C. Horst, L. Aldana, Development and Application of Remote, Near Real-Time Methane Detector Network for Belowground Pipeline Leaks, Energy Institute Student Research Poster Session at Powerhouse, Colorado State University, May 10, 2022 (Poster).
10. **Smits, K.M.** Quantification of anthropogenic methane sources through measurement studies: Finding targets for mitigation, SMU Earth Science Seminar Series, Jan 27, 2023 **(Invited Presentation).**
11. **Smits, K.M.** Unraveling the Influence of Environmental Conditions on Natural Gas Pipeline Leak Behavior, Center for Energy and Environmental Resources (CEER), The University of Texas at Austin, March 7, 2022 **(Invited Presentation).**
12. **Smits, K.M**., D. Zimmerle, Y. Cho, S. Riddick, B. Gao and S. Tian, Unraveling the influence of environmental parameters on methane behavior from belowground leaks, American Geophysical Union Fall Meeting, Dec 2021 **(Presentation)**.
13. **Smits, K.M.**, Tools for Predicting Underground Natural Gas Migration and Mitigating its Occurrence/Consequence, School of Global Environmental Sustainability, Colorado State University, Dec 6, 2021 **(Invited Presentation).**

Media Reports

1. Agor, J., 2020. "Monitoring gas leaks UTA civil engineering working to develop data network to monitor, quantify gas leaks." https://www.uta.edu/news/news-releases/2020/10/05/smits-gas-leaks Published on 5 October, 2020.
2. Agor, J., 2021, "UTA civil engineering professor earns grants to study, develop methods to assess and respond to large gas leaks," Jan 2021, https://www.uta.edu/news/news-releases/2021.
3. Rumende, Thevnin. "Civil engineering professor receives two grants to study natural gas leak detection methods," The Shorthorn, Published on February 11, 2021, https://www.theshorthorn.com/news/civil-engineering-professor-receives-two-grants-to-study-natural-gas-leak-detection-methods/article_9d943c92-6cd2-11eb-96be-832c69a5f352.html

Data

Jui-Hsiang Lo; Kathleen M Smits; Younki Cho; Gerald P. Duggan; Stuart Riddick, 2023, "Replication Data for: Quantifying Non-steady State Natural Gas Leakage from the Pipelines Using an Innovative Sensor Network and Model for Subsurface Emissions - InSENSE", https://doi.org/10.18738/T8/SPE8QJ, Texas Data Repository, DRAFT VERSION

Workforce Development

- Opportunities for postdoctoral and student training and development were provided as part of this work. 1 postdoctoral researcher, 2 graduate and 5 undergraduate engineering students from diverse backgrounds were supported, in part, by this research. Students/post doc went on to persue positions in various engineering firms (4) and continuing graduate studies (4).

  Graduate and Undergraduate students supported, in part, by this research

Postdoc/Student and affliliation	**Current Employment**
Younki Cho (postdoctoral researcher, Civil Engineering, UTA)	Oil & Gas Engineering firm
Rayson Lo (graduate student, Civil Engineering, CSU)	Graduate Student
Coner Cunningham (graduate student, Mechanical Engineering, CSU)	Engineering firm
Riley Durham (undergraduate student, Mechanical Engineering, CSU)	Engineering/ Research firm
Hilton Duong (undergraduate student, Civil Engineering, UTA)	Graduate student
Nathan Steadman (undergraduate student, Civil Engineering, UTA)	Graduate student, followed by engineering firm

Chandler Horst (undergraduate student, Mechanical Engineering, CSU)	Engineering firm
Luke Aldana (undergraduate student, Electrcial and Computer EngineeringCSU)	Engineering firm

Publications

Publication	**Objective**	**Results/Importance**
Cho, Y., Smits, K. M., Riddick, S. N., & Zimmerle, D. J. (2022). Calibration and field deployment of low-cost sensor network to monitor underground pipeline leakage. Sensors and Actuators B: Chemical, 355, 131276., https://doi.org/10.1016/j.snb.2021.131276	Development and calibration of NG detection unit using low-cost MOS sensors and field deployment of prototype units	*MOS sensors can measure methane concentrations in the 100 - 10,000 ppmv range while monitoring underground leaks
		*Data measured at high spatiotemporal resolution provides an effective monitoring option for the variability in gas concentrations due to environmental conditions
		*An identified leak can be continuously remotely monitoredby low-cost sensors, reporting innear real time, for an extended period
J. Lo*, K.M. Smits, Y. Cho, J. Duggan, S. Riddick, Quantifying Non-steady State Natural Gas Leakage from the Pipelines Using An Innovative Sensor Network and Model for Subsurface missions – InSENSE, *in review*	Estimating the non-steady belowground NG leak rates by the modified gas migration model (the modified ESCAPE model) using surface and belowground near-surface CH_4 measurements, meteorological data, and soil moisture and temperature data.	*Difference of evolution between surface and belowground near-surface CH_4 with the increased gas leak rates highlighted the importance of belowground CH_4 measurement and soil characteristics in the detection and quantification of non-steady belowground NG leak rates.
		* Integrating the belowground soil characteristics and gas measurements with the atmospheric variability could advance the quantification of non-steady belowground NG leak rates.
		* Required number of detectors in the low-cost near-real-time CH_4 detector network to quantify the underground non-steady NG leak rates was 3.

Reference

[1] Bittelli, M., Ventura, F., Campbell, G. S., Snyder, R. L., Gallegati, F., & Pisa, P. R. (2008). Coupling of heat, water vapor, and liquid water fluxes to compute evaporation in bare soils. *Journal of Hydrology, 362*(3-4), 191-205.

[2] Camillo, P. J., & Gurney, R. J. (1986). A resistance parameter for bare-soil evaporation models. *Soil Science, 141*(2), 95-105.

[3] Cho, Y., Smits, K. M., Riddick, S. N., & Zimmerle, D. J. (2022). Calibration and field deployment of low-cost sensor network to monitor underground pipeline leakage. *Sensors and Actuators B: Chemical, 355*, 131276.

[4] Cho, Y., Ulrich, B. A., Zimmerle, D. J., & Smits, K. M. (2020). Estimating natural gas emissions from underground pipelines using surface concentration measurements☆. *Environmental Pollution, 267*, 115514.

[5] Deepagoda, T. C., Smits, K. M., & Oldenburg, C. M. (2016). Effect of subsurface soil moisture variability and atmospheric conditions on methane gas migration in shallow subsurface. *International Journal of Greenhouse Gas Control, 55*, 105-117.

[6] Denmead, O. (2008). Approaches to measuring fluxes of methane and nitrous oxide between landscapes and the atmosphere. *Plant and Soil, 309*(1-2), 5-24.

[7] Dlugokencky, E. (2019). Trends in Atmospheric Methane (www. esrl. noaa. gov/gmd/ccgg/trends_ch4/). NOAA. In: ESRL.

[8] Flesch, T. Wilson, and DJ, Yee, E., 1995, Backward-time Lagrangian stochastic dispersion models and their application to estimate gaseous emissions. *J. App. Meteorol, 34*, 1320.

[9] Hirst, B., Jonathan, P., del Cueto, F. G., Randell, D., & Kosut, O. (2013). Locating and quantifying gas emission sources using remotely obtained concentration data. *Atmospheric environment, 74*, 141-158.

[10] Iwaszenko, S., Kalisz, P., Słota, M., & Rudzki, A. (2021). Detection of natural gas leakages using a laser-based methane sensor and uav. *Remote Sensing, 13*(3), 510.

[11] Li, Z. (2020). *Water and heat transport in shallow subsurface soil and across the soil-air interface: simulation, experiments and parameterization.* Colorado School of Mines,

[12] Lu, B., & He, Y. (2017). Species classification using Unmanned Aerial Vehicle (UAV)-acquired high spatial resolution imagery in a heterogeneous grassland. *ISPRS Journal of Photogrammetry and Remote Sensing, 128*, 73-85.

[13] Millington, R. (1959). Gas diffusion in porous media. *Science, 130*(3367), 100-102.

[14] Millington, R., & Quirk, J. (1960). Transport in porous media. p. 97–106. FA Van Beren et

al.(ed.) Trans. Int. Congr. of Soil Sci., 7th, Madison, WI. 14–24 Aug. 1960. Vol. 1. Elsevier, Amsterdam. *Transport in porous media. p. 97–106. In FA Van Beren et al.(ed.) Trans. Int. Congr. of Soil Sci., 7th, Madison, WI. 14–24 Aug. 1960. Vol. 1. Elsevier, Amsterdam.*, -.

[15] Moldrup, P., Olesen, T., Gamst, J., Schjønning, P., Yamaguchi, T., & Rolston, D. (2000). Predicting the gas diffusion coefficient in repacked soil water-induced linear reduction model. *Soil Science Society of America Journal, 64*(5), 1588-1594.

[16] Murvay, P.-S., & Silea, I. (2012). A survey on gas leak detection and localization techniques. *Journal of Loss Prevention in the Process Industries, 25*(6), 966-973.

[17] National Academies of Sciences, EM, 2022. Nat. Gas. Available at: Accessed 14 May 2022.

[18] Neirynck, J., Kowalski, A., Carrara, A., Genouw, G., Berghmans, P., & Ceulemans, R. (2007). Fluxes of oxidised and reduced nitrogen above a mixed coniferous forest exposed to various nitrogen emission sources. *Environmental Pollution, 149*(1), 31-43.

[19] Nemitz, E., Sutton, M. A., Schjoerring, J. K., Husted, S., & Wyers, G. P. (2000). Resistance modelling of ammonia exchange over oilseed rape. *Agricultural and Forest Meteorology, 105*(4), 405-425.

[20] PHMSA. Pipeline Incident 20 Year Trends. https://www.phmsa.dot.gov/data-and-statistics/pipeline/pipeline-incident-20-year-trends (accessed March 20, 2020).

[21] Ravikumar, A. P., Wang, J., & Brandt, A. R. (2017). Are optical gas imaging technologies effective for methane leak detection? *Environmental science & technology, 51*(1), 718-724.

[22] Rella, C. W., Tsai, T. R., Botkin, C. G., Crosson, E. R., & Steele, D. (2015). Measuring emissions from oil and natural gas well pads using the mobile flux plane technique. *Environmental science & technology, 49*(7), 4742-4748.

[23] Riddick, S. N., Bell, C. S., Duggan, A., Vaughn, T. L., Smits, K. M., Cho, Y., . . . Zimmerle, D. J. (2021). Modeling temporal variability in the surface expression above a methane leak: The ESCAPE model. *Journal of Natural Gas Science and Engineering, 96*, 104275.

[24] Riddick, S. N., Connors, S., Robinson, A. D., Manning, A. J., Jones, P. S., Lowry, D., . . . Pitt, J. (2017). Estimating the size of a methane emission point source at different scales: from local to landscape. *Atmospheric Chemistry and Physics, 17*(12), 7839-7851.

[25] Riddick, S. N., Mauzerall, D. L., Celia, M., Harris, N. R., Allen, G., Pitt, J., . . . Lowry, D. (2019). Methane emissions from oil and gas platforms in the North Sea. *Atmospheric Chemistry and Physics, 19*(15), 9787-9796.

[26] Schuepp, P. H. (1977). Turbulent transfer at the ground: On verification of a simple predictive model. *Boundary-Layer Meteorology, 12*(2), 171-186.

[27] Seinfeld, J. H., & Pandis, S. N. (2016). *Atmospheric chemistry and physics: from air pollution*

to climate change: John Wiley & Sons.

[28] Sun, S.-F. (1982). Moisture and heat transport in a soil layer forced by atmospheric conditions. *MS Thesis, University of Connecticut*.

[29] Sutton, M., Burkhardt, J., Guerin, D., Nemitz, E., & Fowler, D. (1998). Development of resistance models to describe measurements of bi-directional ammonia surface–atmosphere exchange. *Atmospheric Environment, 32*(3), 473-480.

[30] U.S. Energy Information Administration, 2022. Annual U.S. Natural Gas Production (1940-2020). Available at: Accessed 27 May 2022

[31] Ulrich, B. A., Mitton, M., Lachenmeyer, E., Hecobian, A., Zimmerle, D., & Smits, K. M. (2019). Natural gas emissions from underground pipelines and implications for leak detection. *Environmental Science & Technology Letters, 6*(7), 401-406.

[32] van de Griend, A. A., & Owe, M. (1994). Bare soil surface resistance to evaporation by vapor diffusion under semiarid conditions. *Water Resources Research, 30*(2), 181-188.

[33] Yacovitch, T. I., Herndon, S. C., Pétron, G., Kofler, J., Lyon, D., Zahniser, M. S., & Kolb, C. E. (2015). Mobile laboratory observations of methane emissions in the Barnett Shale region. *Environmental Science & Technology, 49*(13), 7889-7895.

[34] Zhang, H., Lindberg, S. E., Barnett, M. O., Vette, A. F., & Gustin, M. S. (2002). Dynamic flux chamber measurement of gaseous mercury emission fluxes over soils. Part 1: simulation of gaseous mercury emissions from soils using a two-resistance exchange interface model. *Atmospheric Environment, 36*(5), 835-846.

[35] D. Zimmerle, A. Felicio B. Santos, and G. P. Duggan, “DC Approximate Models for Modeling Minigrid Systems,” 2018, pp. 1–7, doi: 10.1109/GHTC.2018.8601930.

[36] S. Dufrane, D. Zimmerle, and G. P. Duggan, “Optimization of photovoltaic penetration for a hybrid diesel and photovoltaic micro-grid via means of a cloud forecasting system,” 2017, pp. 1–7, doi: 10.1109/GHTC.2017.8239262.

[37] J. R. Bleem, G. P. Duggan, W. Stainsby, and D. Zimmerle, “PV Modeling as a Community Resource,” *ASES National Solar Conference 2019*, p. 9.

[38] G. P. Duggan and P. Young, “Precision timing on low-cost Linux microcomputers,” in *2015 Annual IEEE Systems Conference (SysCon) Proceedings*, 2015, pp. 469–471, doi: 10.1109/SYSCON.2015.7116795.